USAXS/SAXS from Organic Pigment Samples

August 2014

Dr. Greg Beaucage, University of Cincinnati
Ms. Hanqiu Jiang, PhD Student, University of Cincinnati
Dr. Karsten Vogtt, Post Doctoral Scientist, University of Cincinnati
Dr. Jan Ilavsky, Scientist, Argonne National Laboratory
Department of Chemical and Materials Engineering, University of Cincinnati, Cincinnati OH 45221-0012, 513 373 3454, beaucag@uc.edu, gbeaucage@gmail.com

Outline:

-Example Fit

-Table of Fit Results for 0.05% Samples

-Plots for Concentration Series and 1μm Films on Mylar

-Plots of Sample Groups for Comparison

-Summary

Samples Run at APS August 2014

		% Pigment					MicroTrak Particle Size (nm)		
	Sample Code	0.50%	1.00%	Neat	Gently Dried (2 grams)	Prints on Mylar	D10	D50	D95
1	PR179-E-Control	PR179-E-C-0.5	PR179-E-C-1	PR179-E-C-N	PR179-E-C-D	PR179-E-C	29.6	101.0	196.0
2	PR179-Eb	PR179-Eb-0.5	PR179-Eb-1	PR179-Eb-N	PR179-Eb-D	PR179-Eb	109.8	180.5	330.0
3	PB15:1-E-Control	PB15:1-E-C-0.5	PB15:1-E-C-1	PB15:1-E-C-N	PB15:1-E-C-D	PB15:1-E-C	148.3	358.0	704.0
4	PB15:1-Eb	PB15:1-Eb-0.5	PB15:1-Eb-1	PB15:1-Eb-N	PB15:1-Eb-D	PB15:1-Eb	139.4	271.8	623.0
5	PB15:3-P-Control	PB15:3-P-C-0.5	PB15:3-P-C-1	PB15:3-P-C-N	PB15:3-P-C-D	PB15:3-P-C	150.3	245.6	389.0
6	PB15:3-RSb	PB15:3-RSb-0.5	PB15:3-RSb-1	PB15:3-RSb-N	PB15:3-RSb-D	PB15:3-RSb	104.3	180.4	332.0
7	PB15:3-RSb-Eb	PB15:3-RSb-Eb-0.5	PB15:3-RSb-Eb-1	PB15:3-RSb-Eb-N	PB15:3-RSb-Eb-D	PB15:3-RSb-Eb	98.7	160.8	283.7
8	PB15:3-M	PB15:3-M-0.5	PB15:3-M-1	PB15:3-M-N	PB15:3-M-D	PB15:3-M	130.2	207.7	348.0
9	PY14-P-Control	PY14-P-C-0.5	PY14-P-C-1	PY14-P-C-N	PY14-P-C-D	PY14-P-C	144.7	275.9	493.0
10	PY14-134%-Pb	PY14-134%-Pb-0.5	PY14-134%-Pb-1	PY14-134%-Pb-N	PY14-134%-Pb-D	PY14-134%-Pb	102.4	166.3	308.0
11	PY14-124%-Pb	PY14-124%-Pb-0.5	PY14-124%-Pb-1	PY14-124%-Pb-N	PY14-124%-Pb-D	PY14-124%-Pb	93.7	193.4	338.0
12	PY14-116%-Pb	PY14-116%-Pb-0.5	PY14-116%-Pb-1	PY14-116%-Pb-N	PY14-116%-Pb-D	PY14-116%-Pb	129.3	214.8	393.0
13	PY14-110%-Pb	PY14-110%-Pb-0.5	PY14-110%-Pb-1	PY14-110%-Pb-N	PY14-110%-Pb-D	PY14-110%-Pb	120.3	212.0	360.0
14	PY14-RSb	PY14-RSb-0.5	PY14-RSb-1	PY14-RSb-N	PY14-RSb-D	PY14-RSb	109.4	200.2	375.0
15	PY14-RSb-Eb	PY14-RSb-Eb-0.5	PY14-RSb-Eb-1	PY14-RSb-Eb-N	PY14-RSb-Eb-D	PY14-RSb-Eb	29.4	113.4	316.0
16	PY-14-M	PY-14-M-0.5	PY-14-M-1	PY-14-M-N	PY-14-M-D	PY-14-M	116.9	198.3	430.0

Example Fit

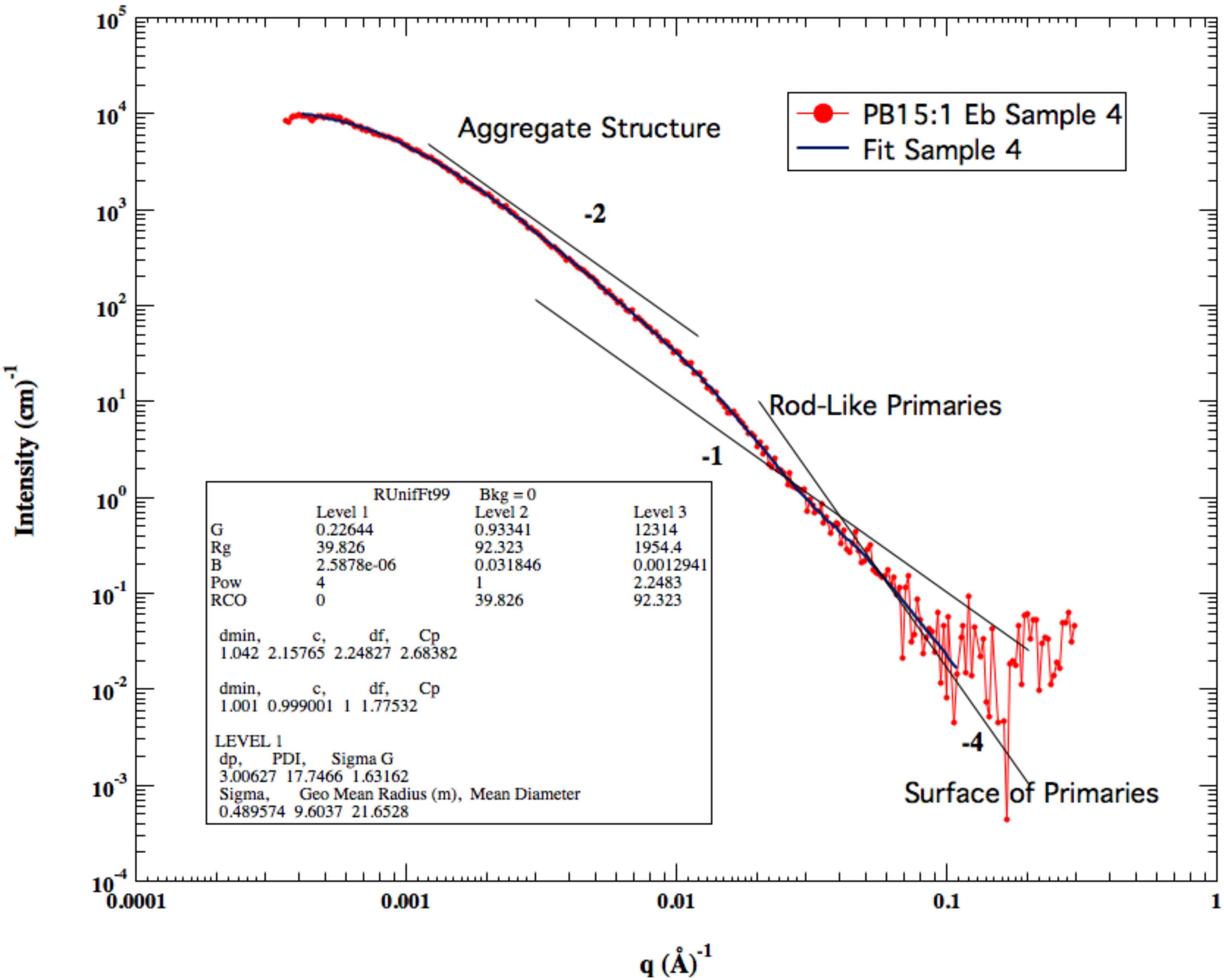

Intensity (cm)$^{-1}$
q (Å)$^{-1}$
PB15:1 Eb Sample 4
Fit Sample 4
Aggregate Structure
-2
-1
Rod-Like Primaries
-4
Surface of Primaries
RUnifFt99 Bkg = 0
Level 1 Level 2 Level 3
G 0.22644 0.93341 12314
Rg 39.826 92.323 1954.4
B 2.5878e-06 0.031846 0.0012941
Pow 4 1 2.2483
RCO 0 39.826 92.323
dmin, c, df, Cp
1.042 2.15765 2.24827 2.68382
dmin, c, df, Cp
1.001 0.999001 1 1.77532
LEVEL 1
dp, PDI, Sigma G
3.00627 17.7466 1.63162
Sigma, Geo Mean Radius (m), Mean Diameter
0.489574 9.6037 21.6528

Fit Results for 0.5% Pigment in Aqueous Surfactant Solution

Sample Number	Sample Code	Level	G, cm-1	±	Rg, Å	±	B, cm-1Å^P	±	P	±	z	±	nBr	±	dmin	c	df	Cp	dp, nm	PDI	SGeo.	Sig, nm	Geo MR, Å	Mn dia, Å	Comments/Assessment	Level	Sample Code	Sample Number
1	PR179-E-Control	1	57	5	132	3	1.07E-06	3.00E-08	4.00										18.2	3.49	1.38	0.32	82.0	173		1	PR179-E-Control	1
		2	1850	30	900	20	0.0020	0.0008	2.15		32.5	3	0	0	1.92	1.12	2.15	1.28								2		
2	PR179-Eb	1	53	7	145	4	7.10E-07	2.00E-08	4.00										19.6	3.61	1.39	0.33	88.3	186	Induced Branching Compared to	1	PR179-Eb	2
		2	4290	50	1030	11	0.0017	0.0007	2.20		80.9	12	10	1	1.31	1.68	2.20	1.37							Control	2		
3	PB15:1-E-Control	1	0.226		39.8		2.59E-06		4.00										3.00	17.7	1.63	0.49	9.6	21.6		1	PB15:1-E-Control	3
		2	0.933		90	30	0.0318		1.00		4.1	0	0	0	1.00	1.00	1.00	1.78							Rod like Primary Particles Aspect 4	2		
		3	39600	800	2550	60	1.66E-03	3.00E-05	2.30	0.00	42400	857	0	0	2.30	1.00	2.30	1.35								3		
4	PB15:1-Eb	1	0.226		39.8		2.59E-06		4.00										3.00	17.7	1.63	0.49	9.6	21.6	Branched Aggregates Compared to	1	PB15:1-Eb	4
		2	0.933		90	30	0.0318		1.00		4.1	0			1.00	1.00	1.00	1.78							Control	2		
		3	12300	300	1950	60	0.0013	0.0002	2.25	0.02	13200	322	4440	104	1.04	2.16	2.25	2.68								3		
5	PB15:3-P-Control	1	33	20	190	11	7.27E-07	2.05E-08	4.00										14.4	19.2	1.64	0.50	44.5	101		1	PB15:3-P-Control	5
		2	88	300	400	100	0.65	0.34	1.00		2.7	11	0	0	1.00	1.00	1.00	1.52							Rod like Primary Particles Aspect 3	2		
		3	14200	200	1600	100	0.015	0.02	1.98	0.20	161.4	552	50	156	1.08	1.83	1.98	2.22							Branched Aggregates	3		
6	PB15:3-RSb	1	140	15	238	8	7.03E-07	2.00E-08	4.00										20.9	9.73	1.55	0.44	81.4	179	Not Rod Like	1	PB15:3-RSb	6
		2	3300	60	890	20	0.00144	0.0008	2.32	0.10	23.6	3	3.64	0.35	1.34	1.73	2.32	2.39							Unbranched	2		
7	PB15:3-RSb-Eb	1	130	10	230	7	7.61E-07	2.00E-08	4.00										20.2	9.81	1.55	0.44	78.5	173	Not Rod Like	1	PB15:3-RSb-Eb	7
		2	3180	80	990	30	0.000148	6.00E-05	2.68	0.07	24.5	2	0.15	0.01	2.09	1.28	2.68	2.61							Unbranched	2		
8	PB15:3-M	1	54	7	187	6	8.54E-07	2.80E-08	4.00										15.5	11.9	1.58	0.45	56.8	126	Not Rod Like	1	PB15:3-M	8
		2	15500	400	1240	30	0.000385	6.00E-05	2.66	0.03	287.0	45	64	9	1.17	2.28	2.66	4.14							Branched Aggregates	2		
9	PY14-P-Control	1	80	20	260	20	2.37E-07	1.00E-08	4.00										24.1	8.2	1.52	0.42	97.7	213	Large Branched Aggregates	1	PY14-P-Control	9
		2	22400	200	1810	20	0.000235	4.00E-05	2.60	0.03	280.0	73	62	14	1.17	2.23	2.60	3.04							Polydisperse	2		
10	PY14-134%-Pb	1	220	70	300	20	3.08E-07	9.00E-09	4.00										30.0	6.67	1.49	0.40	127.0	274	Smaller Aggregates with weak	1	PY14-134%-Pb	10
		2	4900	300	1270	70	0.00207	0.002	2.18	0.13	22.3	8	2.44	0.64	1.42	1.54	2.18	1.86							Branching	2		
		3					8.62E-10	7.00E-12	4.00																Micron Scale Agglomerates	3		
11	PY14-124%-Pb	1	36	7	209	8	3.56E-07	1.00E-08	4.00										17.4	11.8	1.57	0.45	64.0	142	Linear Aggregates Low Polydispersity	1	PY14-124%-Pb	11
		2	6300	100	1320	30	0.00205	0.0004	2.22	0.03	175.0	37	0	0	2.22	1.00	2.22	1.34							Simlar Size to Control	2		
12	PY14-116%-Pb	1	22	7	180	13	3.15E-07	2.00E-08	4.00										16.0	9.92	1.55	0.44	61.9	136	Large Highly Branched Aggs.	1	PY14-116%-Pb	12
		2	8500	100	1230	20	0.000178	3.39E-05	2.67	0.03	386.4	127	149	47	1.05	2.54	2.67	3.86							High polydispersity	2		
13	PY14-110%-Pb	1	27	8	190	10	3.00E-07	2.00E-08	4.00										17.1	9.41	1.54	0.43	67.1	147	Similar to Control with Smaller	1	PY14-110%-Pb	13
		2	5850	70	1060	10	0.000167	5.00E-05	2.67	0.05	216.7	67	76	22	1.08	2.48	2.67	3.59							Primary Particles	2		
14	PY14-RSb	1	9		140	10	4.36E-07	3.00E-08	4.00										11.7	11.2	1.57	0.45	43.6	96.4	Large Aggregates with Few Branches	1	PY14-RSb	14
		2	3080	80	970	30	0.000248	5.00E-05	2.57	0.04	342.2	9	151	4	1.02	2.51	2.57	4.16							Small Primaries	2		
15	PY14-RSb-Eb	1	17	3	145	6	6.11E-07		4.00										12.8	9.67	1.54	0.44	49.7	109	Small Aggregates with Branching	1	PY14-RSb-Eb	15
		2	530	80	800	100	0.00211	0.001	1.96	0.10	31.2	10	5	1.25	1.27	1.55	1.96	1.61							Small Primaries	2		
		3					1.11E-09	9.00E-12	4.00																Micron Scale Agglomerates	3		
16	PY-14-M	1	9	5	150	10	3.48E-07	3.00E-08	4.00										12.3	11.4	1.57	0.45	45.9	101	Large Aggregates with No Branching	1	PY-14-M	16
		2	2410	80	870	30	0.000439	0.0001	2.45	0.06	267.8	158	0	0	2.45	1.00	2.45	1.34							Small Primaries	2		
	Sample Code	Level	G, cm-1	±	Rg, Å	±	B, cm-1Å^P	±	P	±	z	±	nBr	±	dmin	c	df	Cp	dp, nm	PDI	SGeo.	Sig, nm	Geo MR, Å	Mn dia, Å	Comments/Assessment	Level	Sample Code	Sample Number

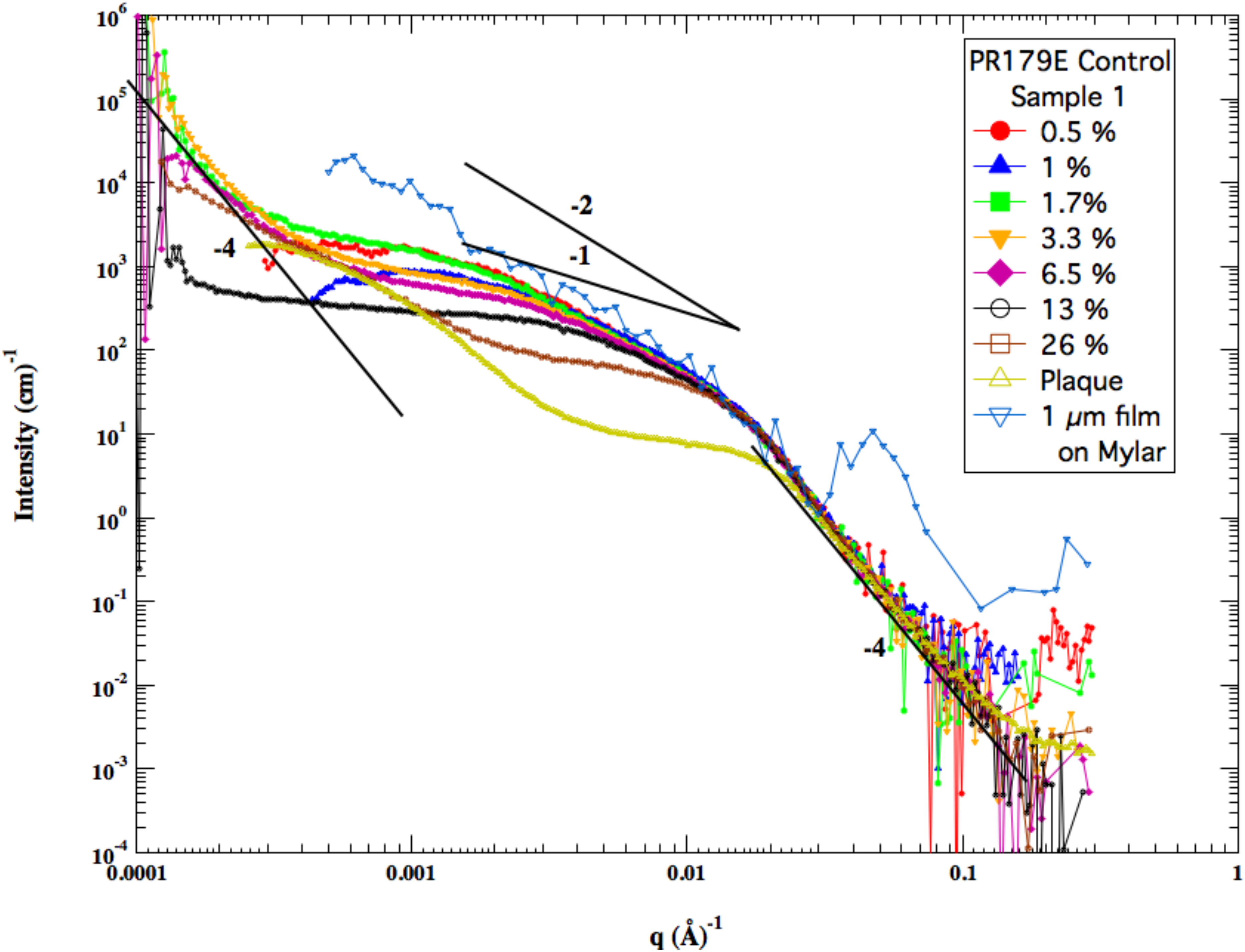

PR179E Control
Sample 1
0.5 %
1 %
1.7%
3.3 %
6.5 %
13 %
26 %
Plaque
1 μm film
on Mylar
-4
-2
-1
-4
Intensity (cm)$^{-1}$
q (Å)$^{-1}$
10^{6}
10^{5}
10^{4}
10^{3}
10^{2}
10^{1}
10^{0}
10^{-1}
10^{-2}
10^{-3}
10^{-4}
0.0001
0.001
0.01
0.1
1

Concentration Series

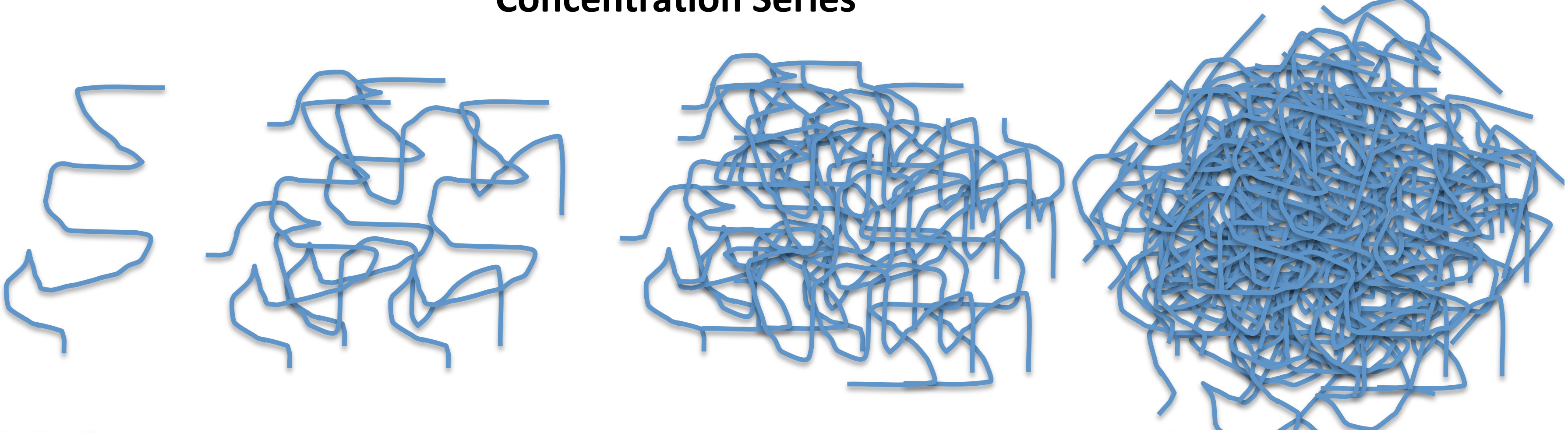

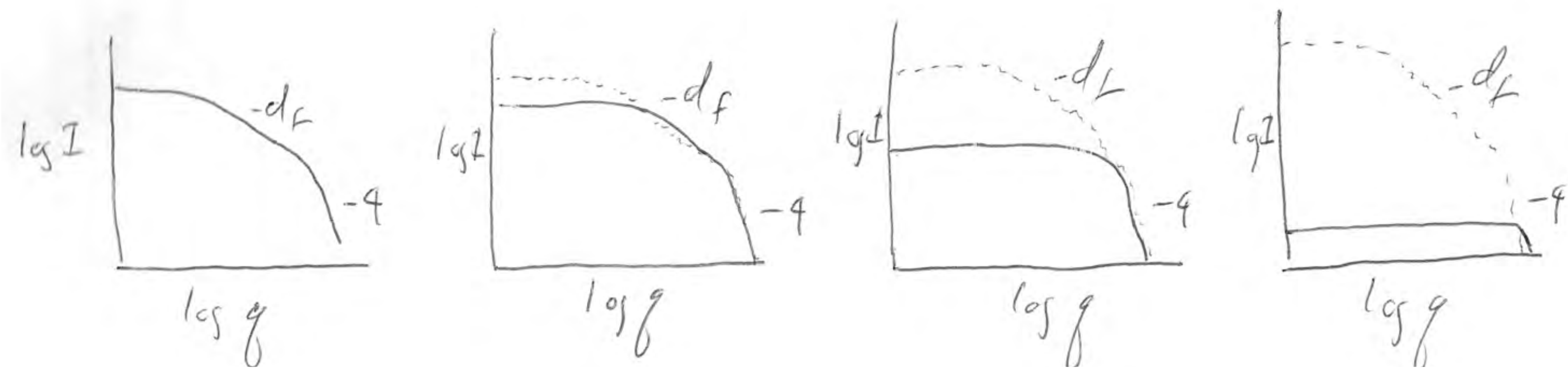

$$1/I(q, \Phi_V) = 1/I(q, \Phi_V=0) + \Phi_V\,(V_{sp}/V_{0,sp})\,(1/(1 - \Phi_V) - 2\chi)/I(q=0, \Phi_V=0) \qquad (3)$$

where χ is an enthalpic interaction between solvent and a subunit of the aggregate, and $(V_{sp}/V_{0,sp})$ is the ratio of the volume of that subunit and the volume of a water molecule. In this case, the subunit is ill defined and we could just consider the more generic second virial coefficient,

$$2A_2 = (1/(1 - \Phi_V) - 2\chi) \qquad (4).$$

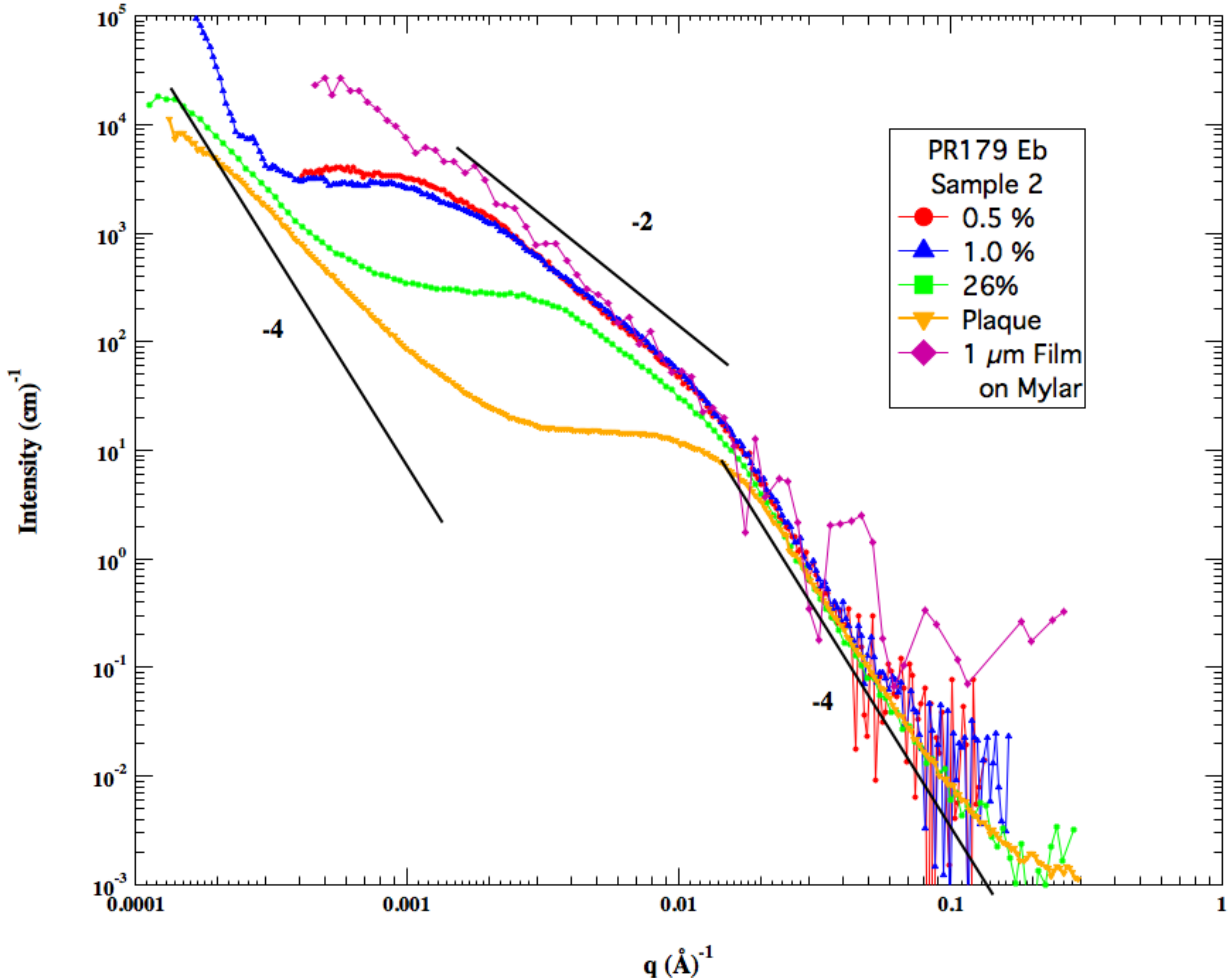
PR179 Eb
Sample 2
0.5 %
1.0 %
26%
Plaque
1 μm Film on Mylar
-2
-4
-4
Intensity (cm)-1
q (Å)-1
10^5
10^4
10^3
10^2
10^1
10^0
10^-1
10^-2
10^-3
0.0001
0.001
0.01
0.1
1

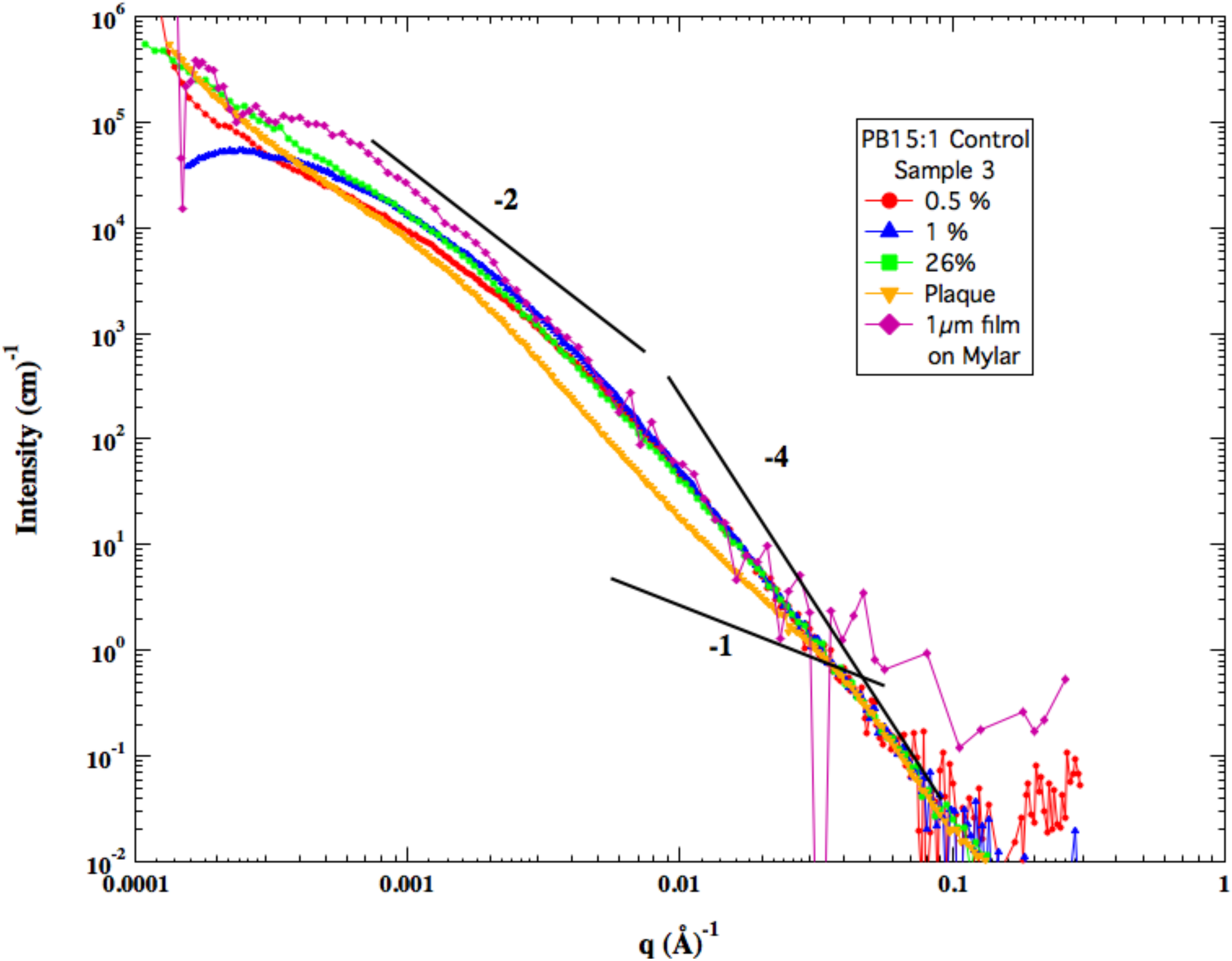

PB15:1 Control
Sample 3
0.5 %
1 %
26%
Plaque
1µm film
on Mylar
-2
-4
-1
Intensity (cm)$^{-1}$
q (Å)$^{-1}$
10^{6}
10^{5}
10^{4}
10^{3}
10^{2}
10^{1}
10^{0}
10^{-1}
10^{-2}
0.0001
0.001
0.01
0.1
1

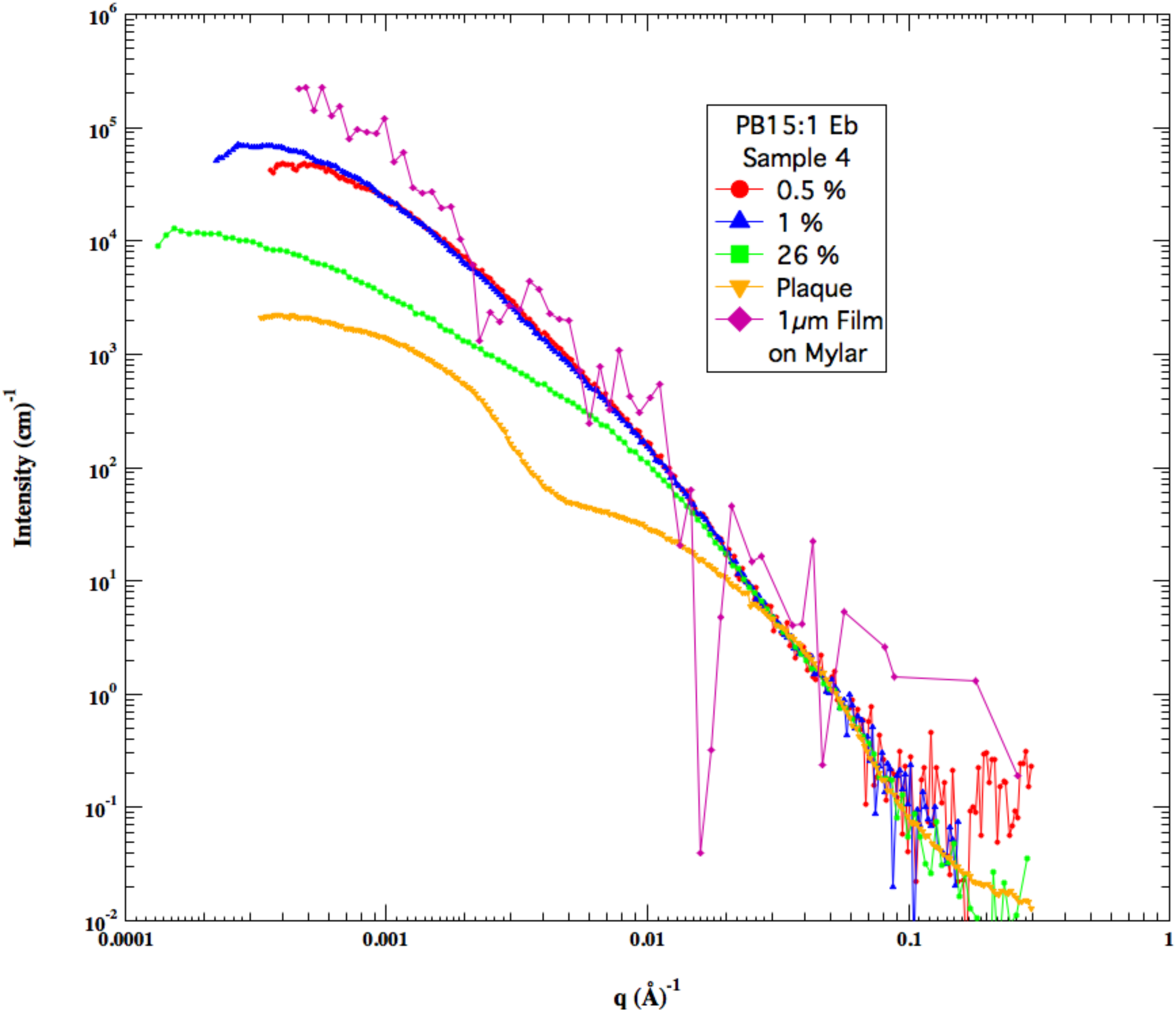

PB15:1 Eb
Sample 4
0.5 %
1 %
26 %
Plaque
1μm Film
on Mylar
Intensity (cm)^-1
q (Å)^-1
10^6
10^5
10^4
10^3
10^2
10^1
10^0
10^-1
10^-2
0.0001
0.001
0.01
0.1
1

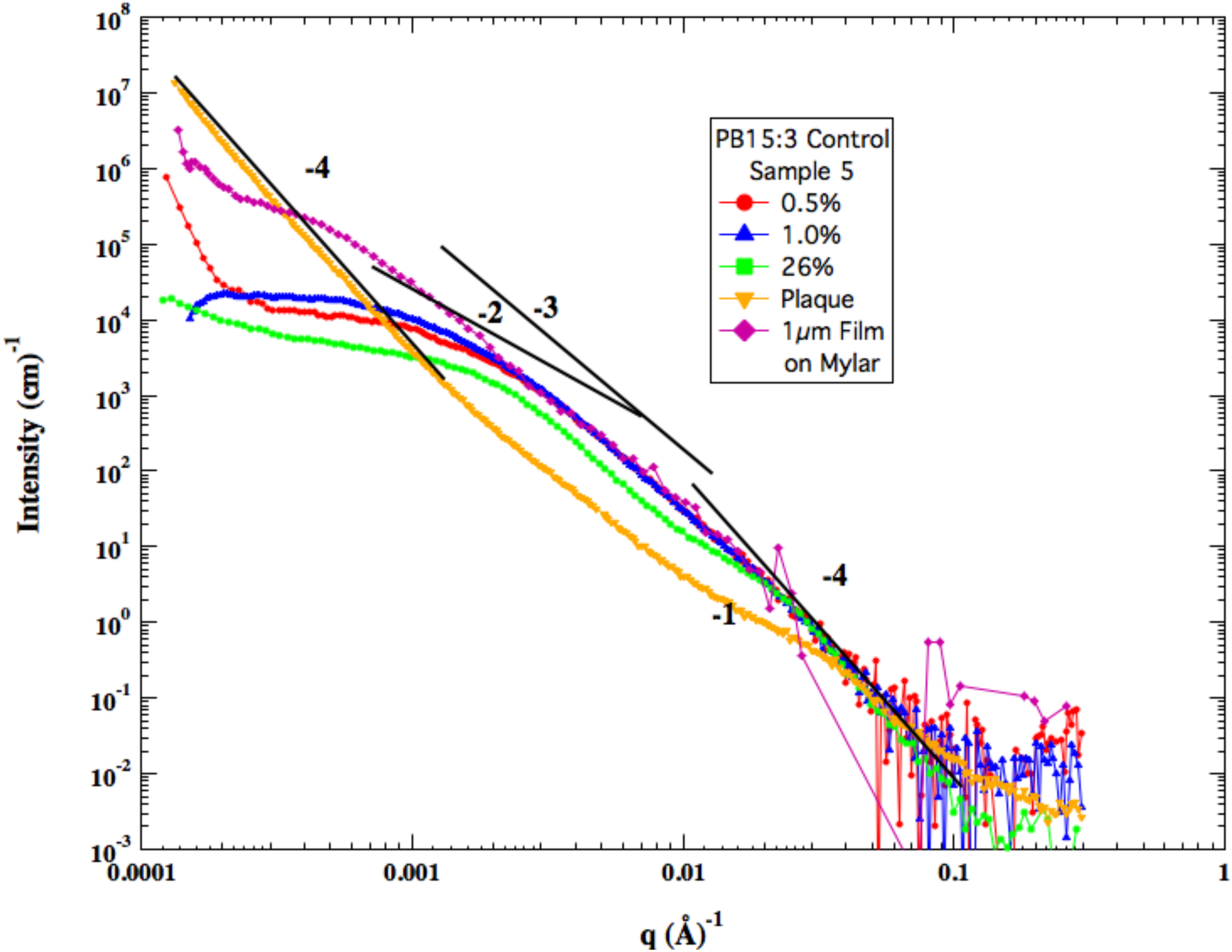
PB15:3 Control
Sample 5
0.5%
1.0%
26%
Plaque
1μm Film
on Mylar
-4
-2
-3
-4
-1
Intensity (cm)-1
q (Å)-1
10^8
10^7
10^6
10^5
10^4
10^3
10^2
10^1
10^0
10^-1
10^-2
10^-3
0.0001
0.001
0.01
0.1
1

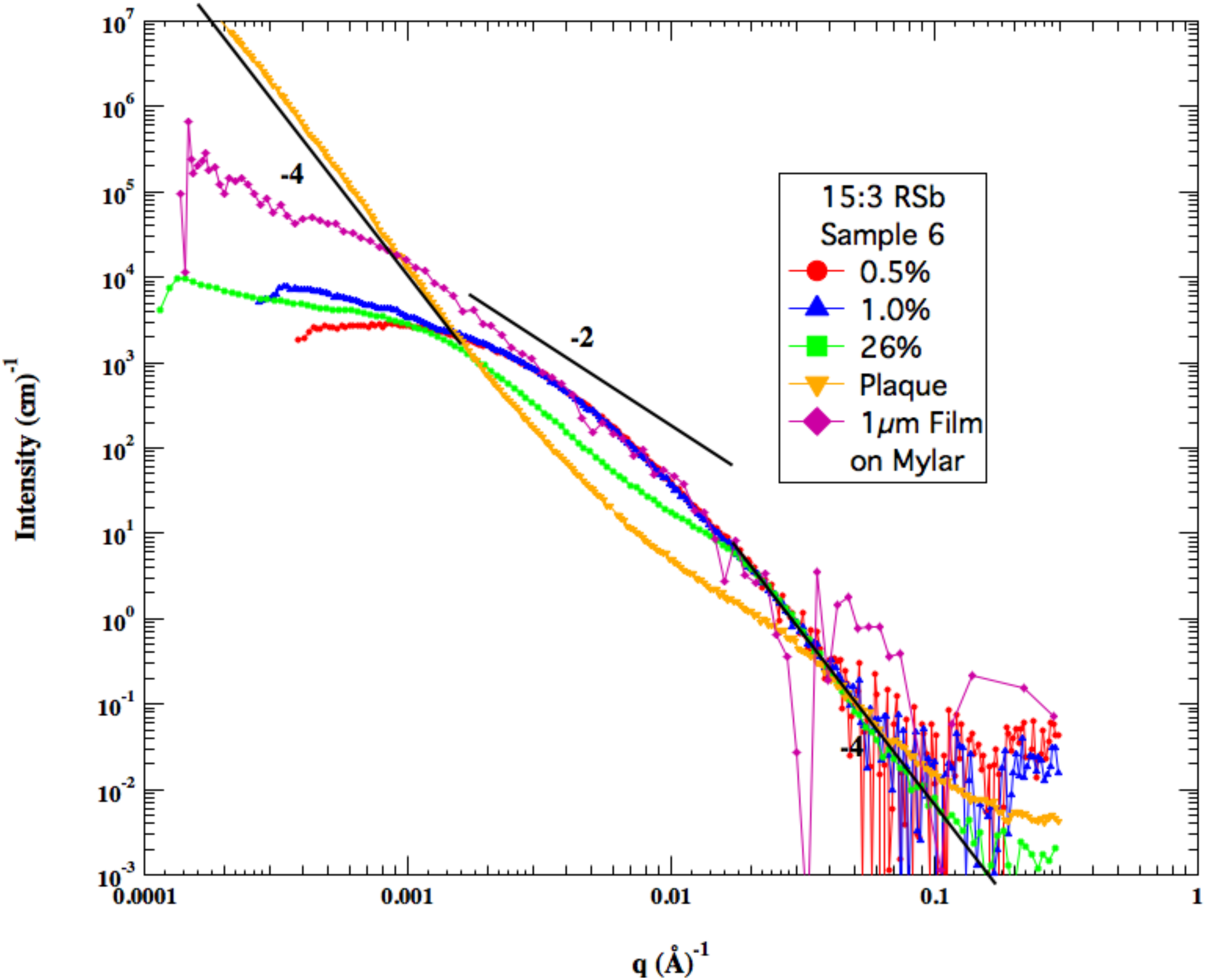
15:3 RSb
Sample 6
0.5%
1.0%
26%
Plaque
1μm Film
on Mylar
-4
-2
-4
Intensity (cm)^-1
q (Å)^-1
0.0001
0.001
0.01
0.1
1

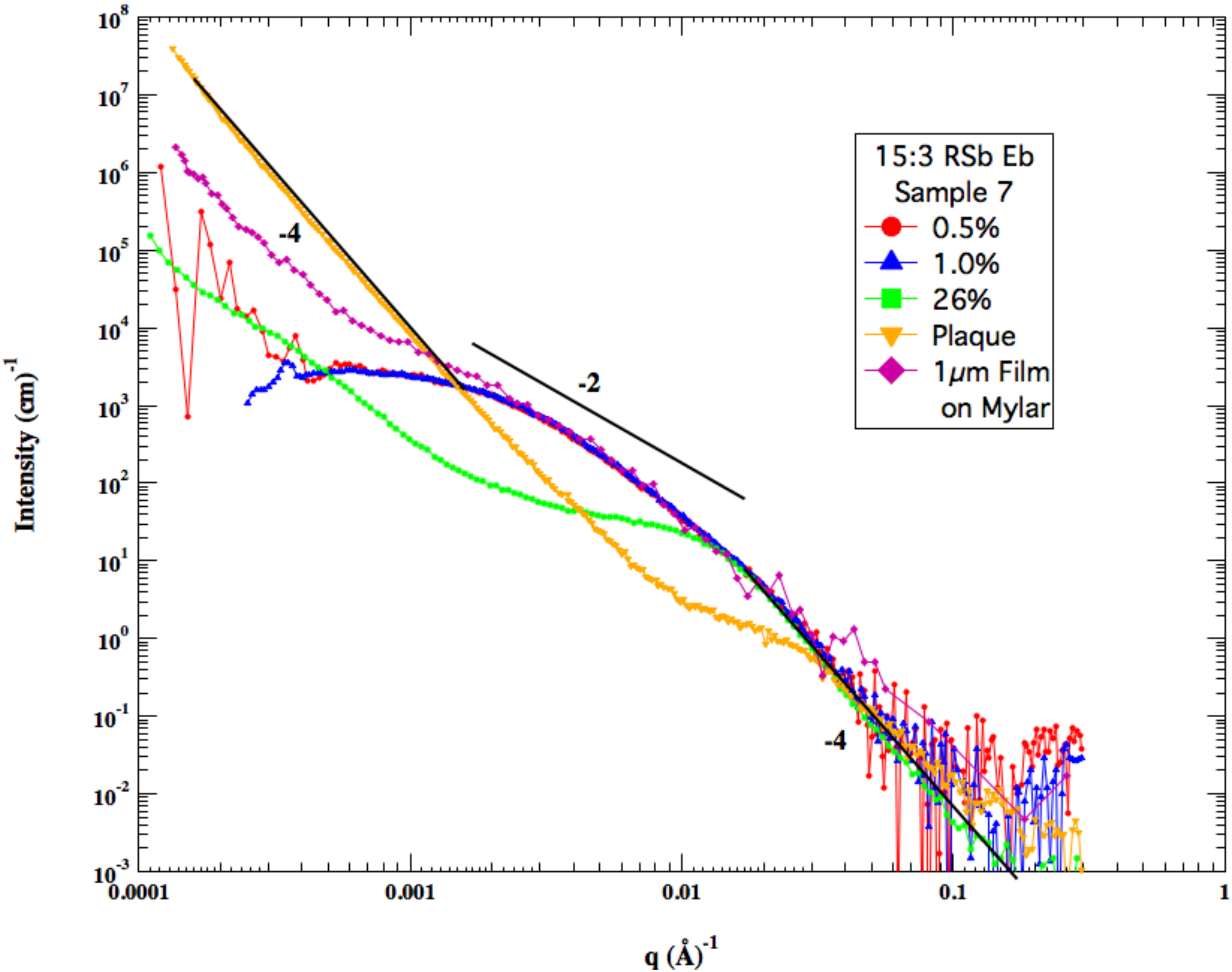

15:3 RSb Eb
Sample 7
0.5%
1.0%
26%
Plaque
1 μm Film
on Mylar
-4
-2
-4
Intensity (cm)-1
q (Å)-1
0.0001
0.001
0.01
0.1
1
10^8
10^7
10^6
10^5
10^4
10^3
10^2
10^1
10^0
10^-1
10^-2
10^-3

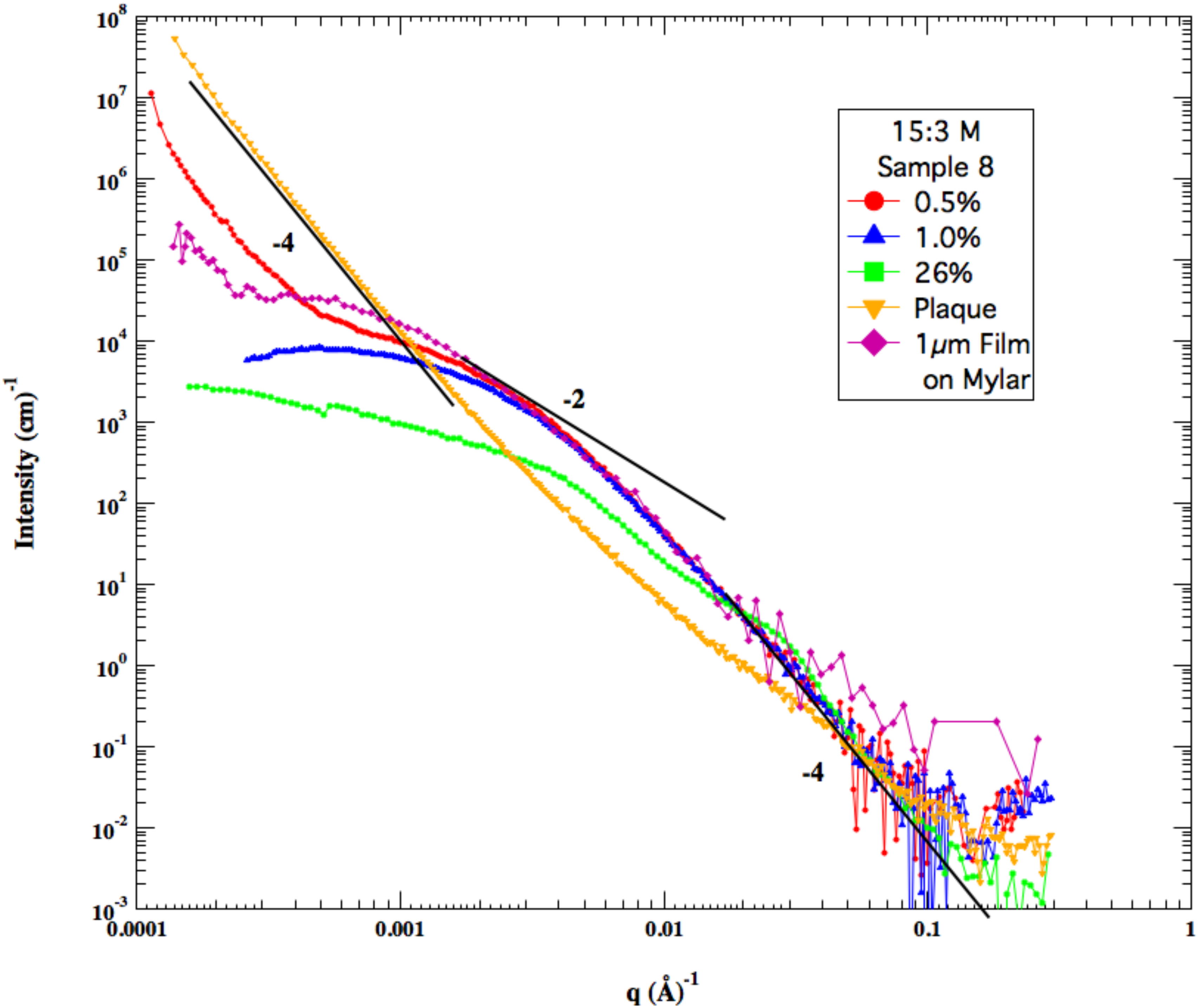

15:3 M
Sample 8
0.5%
1.0%
26%
Plaque
1μm Film
on Mylar
-4
-2
-4
Intensity (cm)-1
q (Å)-1
0.0001
0.001
0.01
0.1
1
10^8
10^7
10^6
10^5
10^4
10^3
10^2
10^1
10^0
10^-1
10^-2
10^-3

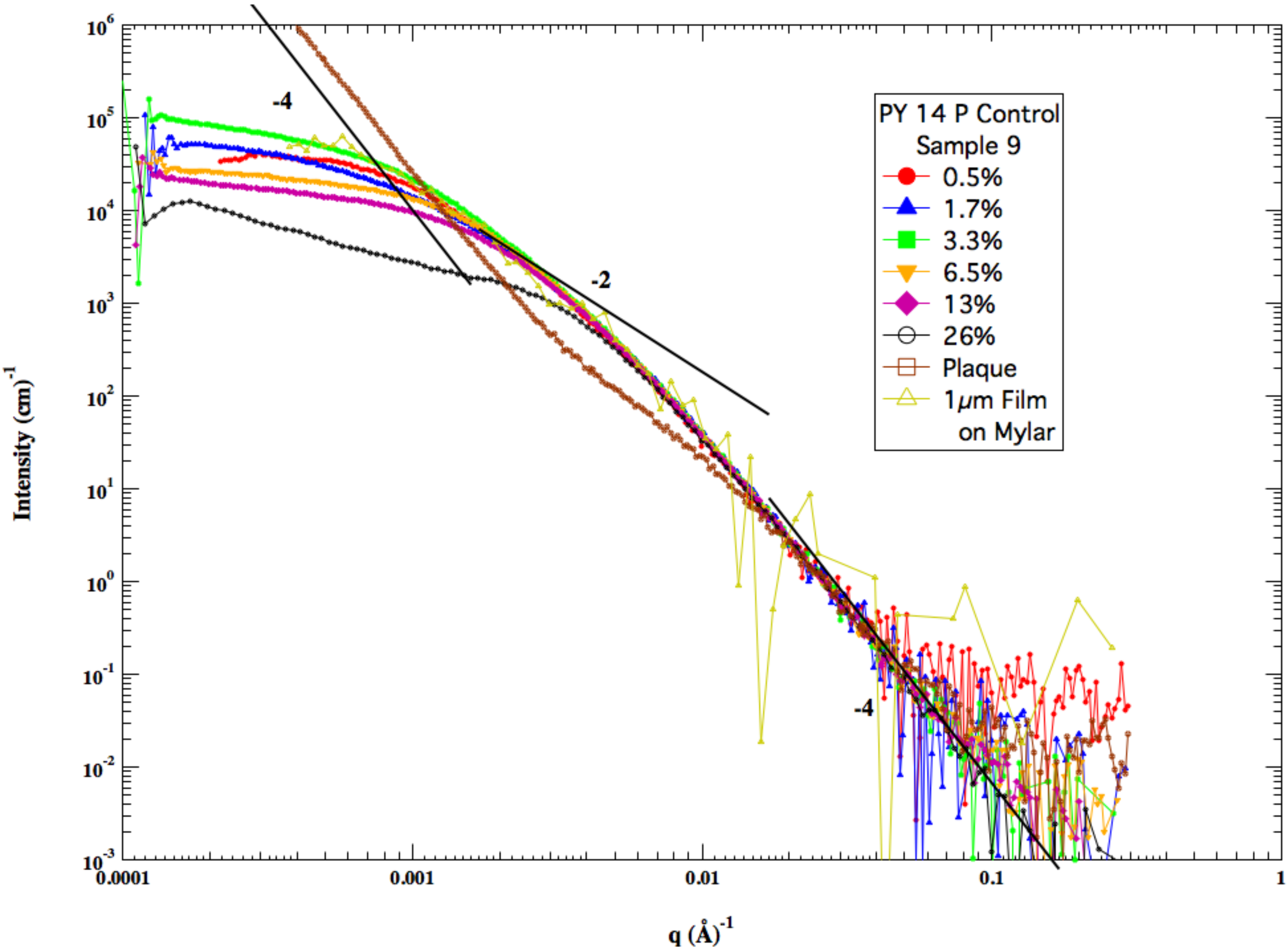

PY 14 P Control
Sample 9
0.5%
1.7%
3.3%
6.5%
13%
26%
Plaque
1μm Film
on Mylar
-4
-2
-4
Intensity (cm)$^{-1}$
q (Å)$^{-1}$
10^{6}
10^{5}
10^{4}
10^{3}
10^{2}
10^{1}
10^{0}
10^{-1}
10^{-2}
10^{-3}
0.0001
0.001
0.01
0.1
1

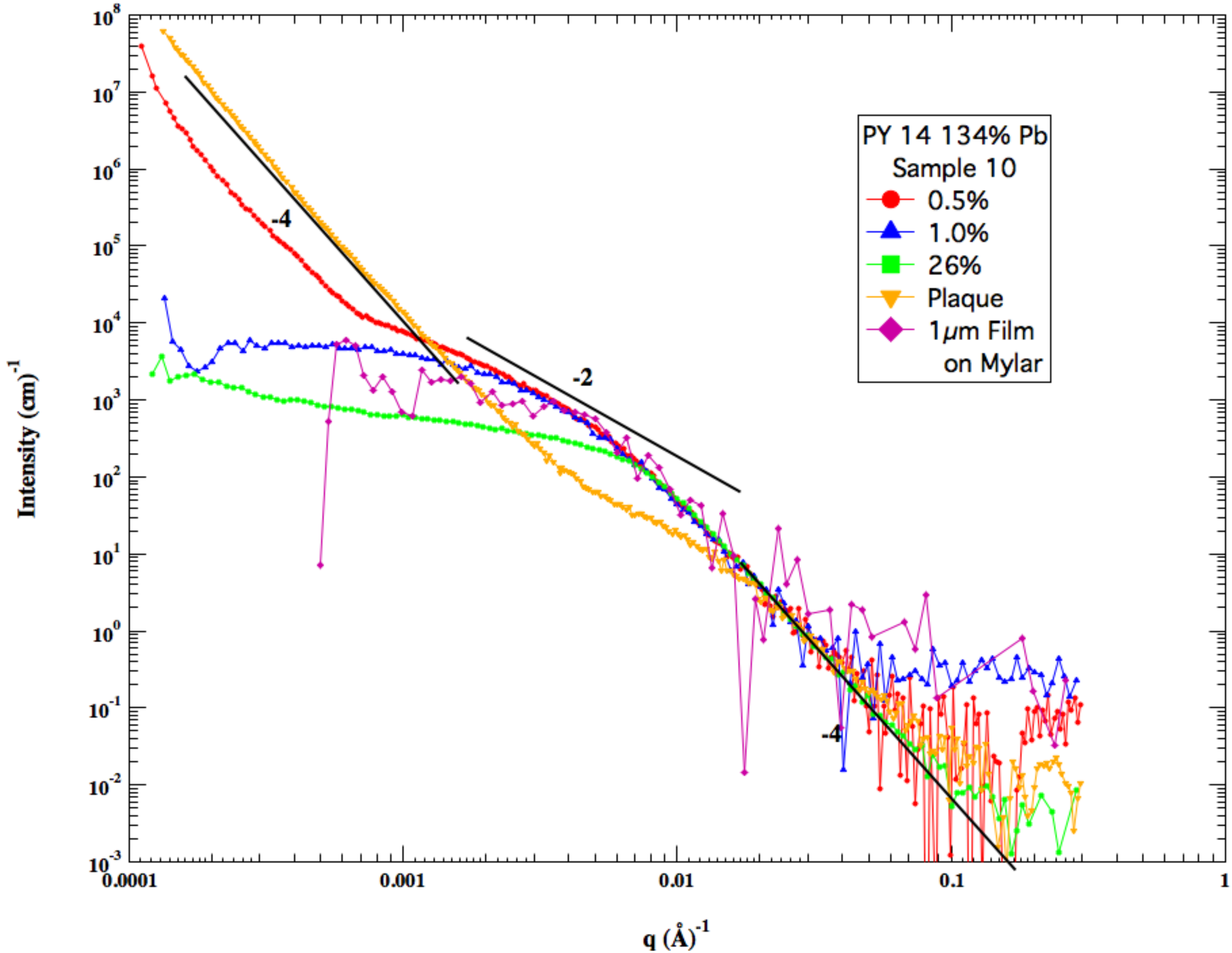

PY 14 134% Pb
Sample 10
0.5%
1.0%
26%
Plaque
1μm Film
on Mylar
-4
-2
-4
Intensity (cm)$^{-1}$
q (Å)$^{-1}$
10^{8}
10^{7}
10^{6}
10^{5}
10^{4}
10^{3}
10^{2}
10^{1}
10^{0}
10^{-1}
10^{-2}
10^{-3}
0.0001
0.001
0.01
0.1
1

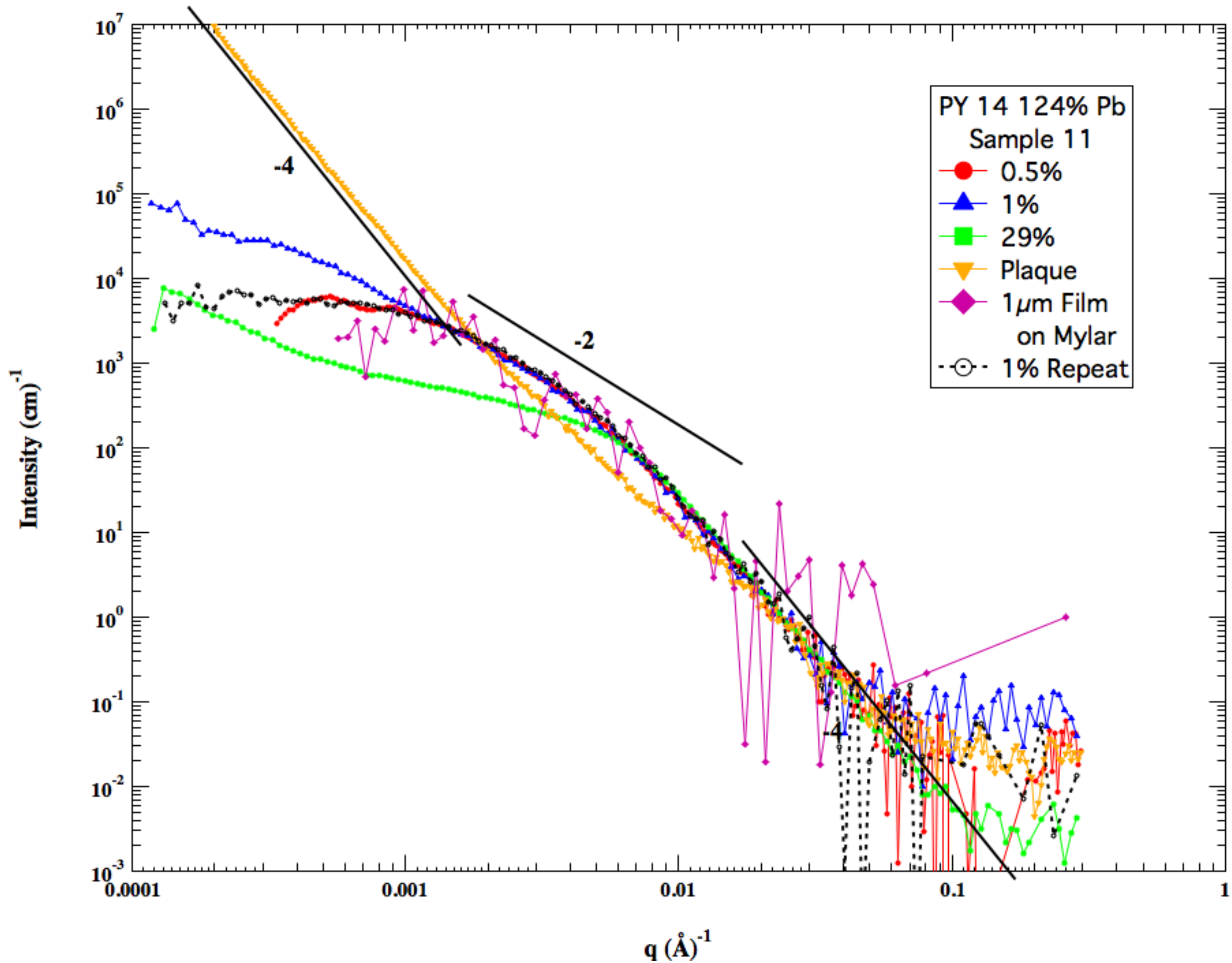
PY 14 124% Pb
Sample 11
0.5%
1%
29%
Plaque
1μm Film on Mylar
1% Repeat
-4
-2
-4
Intensity (cm)$^{-1}$
q (Å)$^{-1}$
10^{7}
10^{6}
10^{5}
10^{4}
10^{3}
10^{2}
10^{1}
10^{0}
10^{-1}
10^{-2}
10^{-3}
0.0001
0.001
0.01
0.1
1

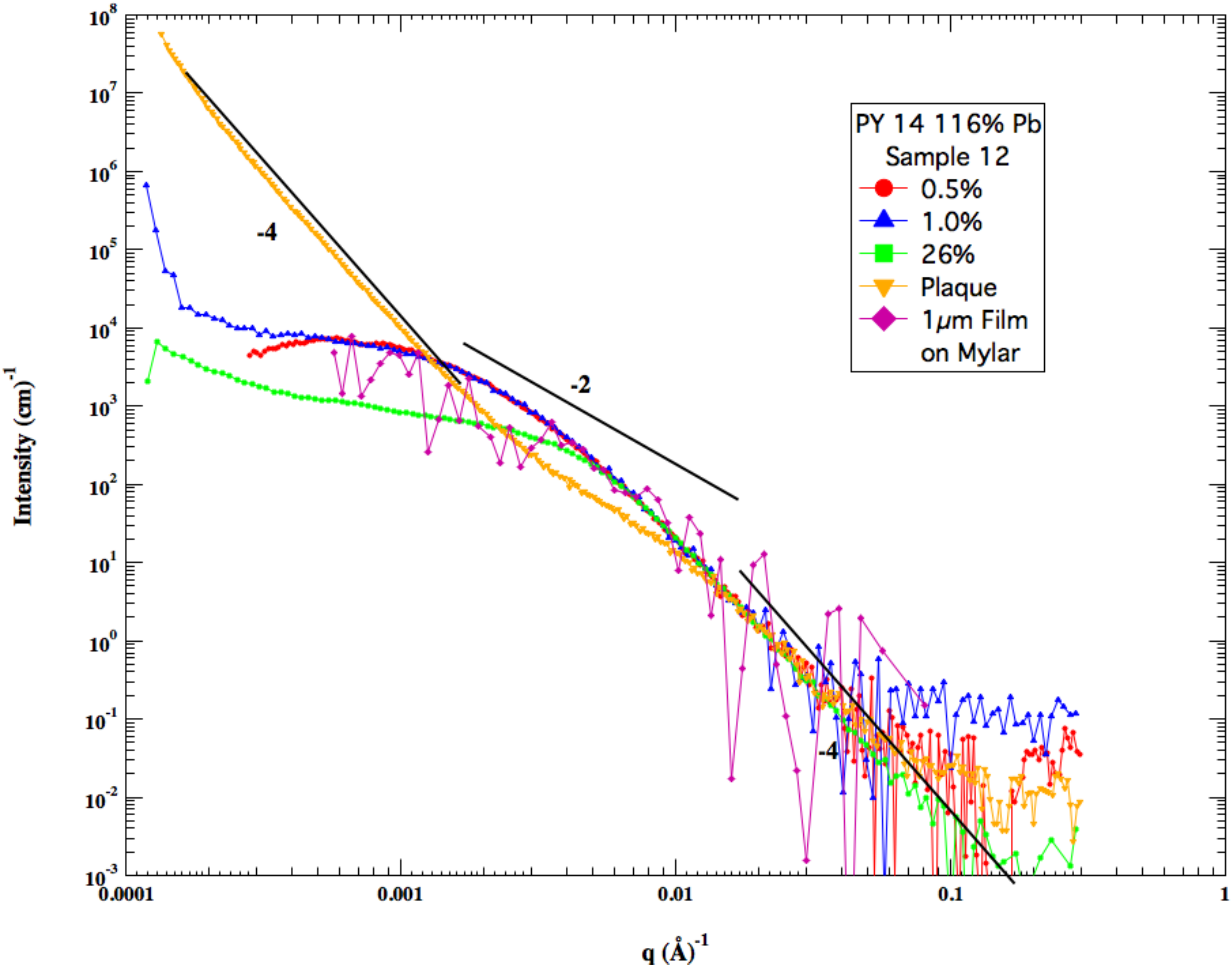
PY 14 116% Pb
Sample 12
0.5%
1.0%
26%
Plaque
1μm Film
on Mylar
-4
-2
-4
Intensity (cm)$^{-1}$
q (Å)$^{-1}$
0.0001
0.001
0.01
0.1
1
10^8
10^7
10^6
10^5
10^4
10^3
10^2
10^1
10^0
10^{-1}
10^{-2}
10^{-3}

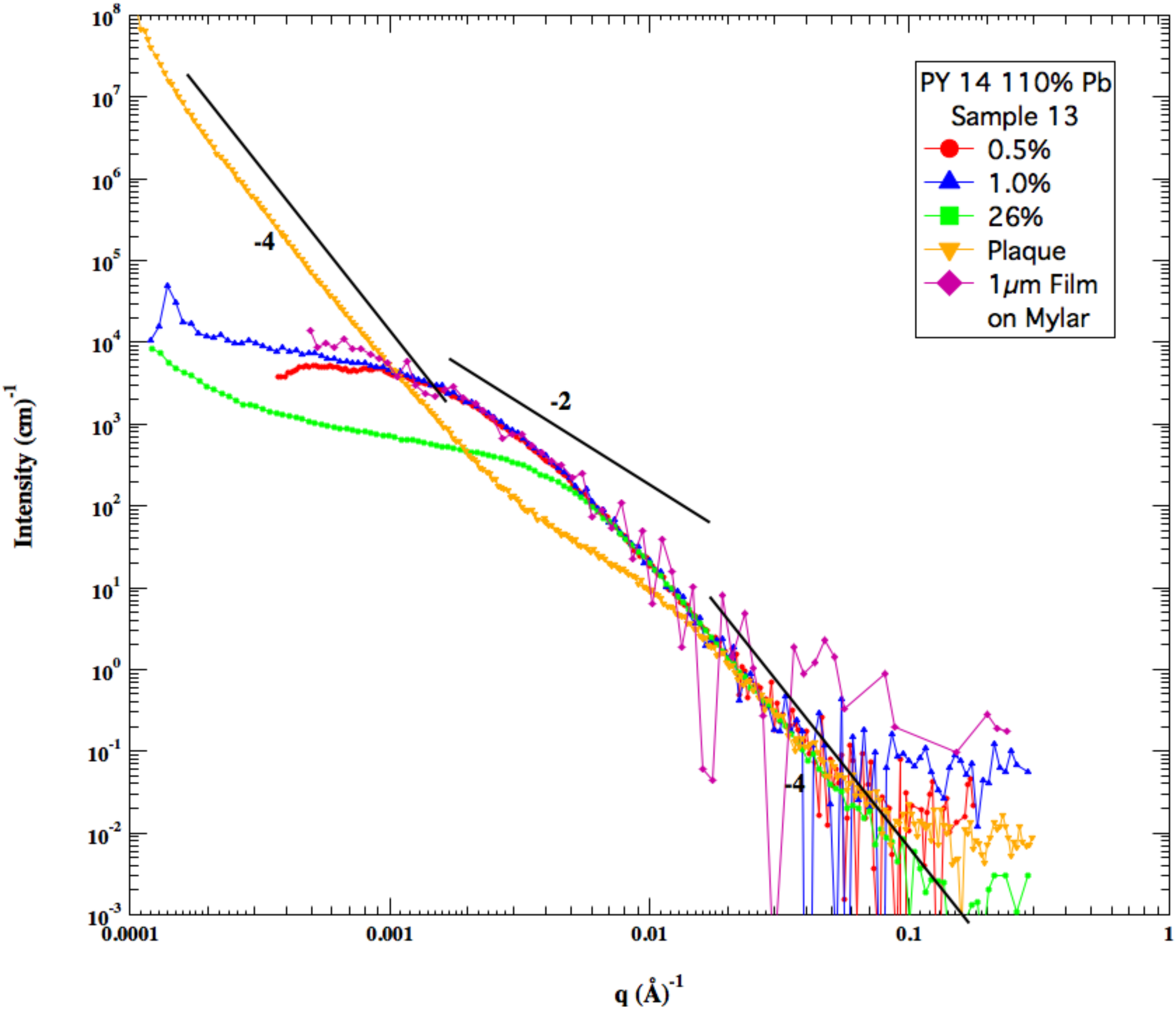
PY 14 110% Pb
Sample 13
0.5%
1.0%
26%
Plaque
1μm Film
on Mylar
-4
-2
-4
Intensity (cm)$^{-1}$
q (Å)$^{-1}$
10^{8}
10^{7}
10^{6}
10^{5}
10^{4}
10^{3}
10^{2}
10^{1}
10^{0}
10^{-1}
10^{-2}
10^{-3}
0.0001
0.001
0.01
0.1
1

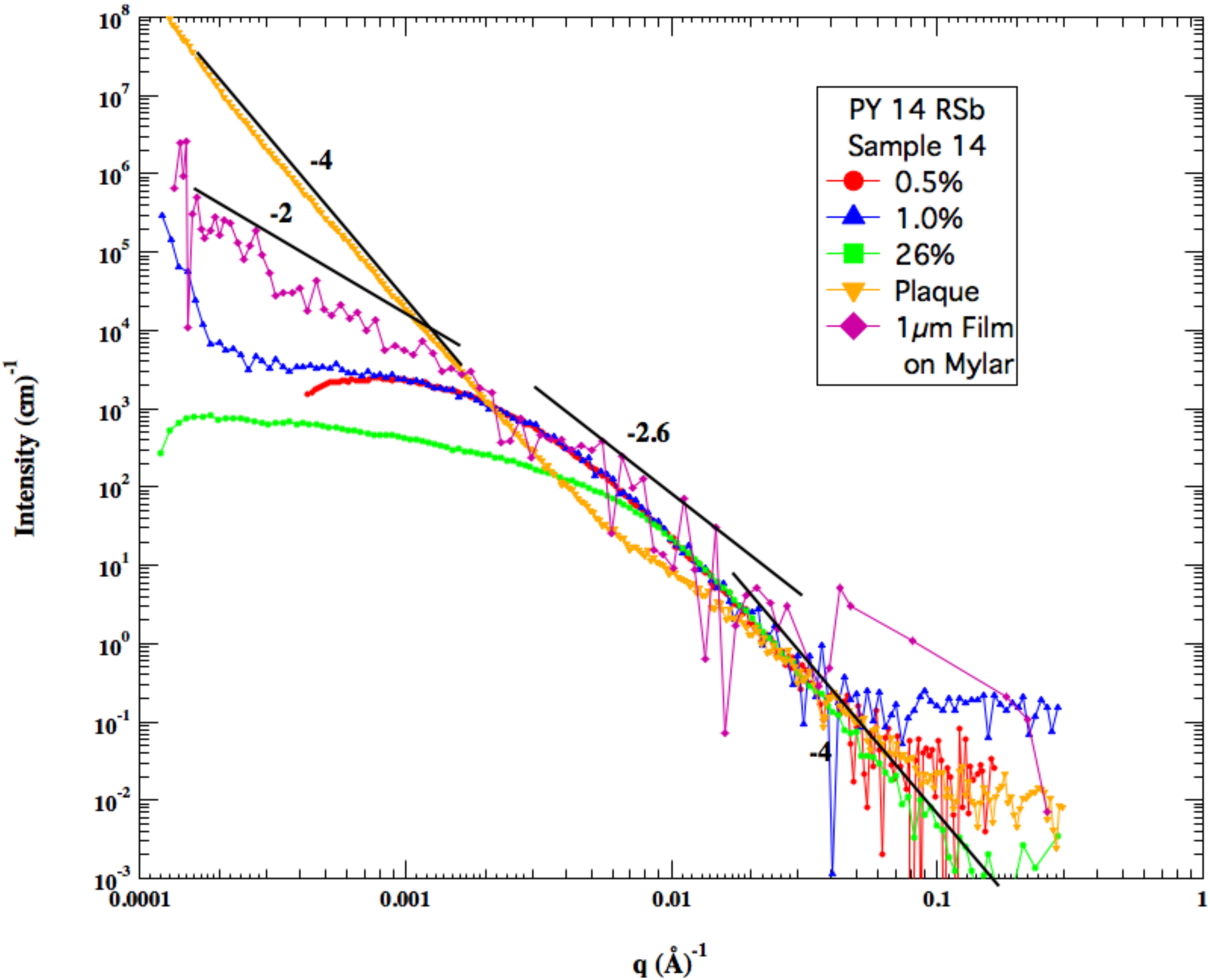

PY 14 RSb
Sample 14
0.5%
1.0%
26%
Plaque
1μm Film on Mylar
-4
-2
-2.6
-4
Intensity (cm)-1
q (Å)-1

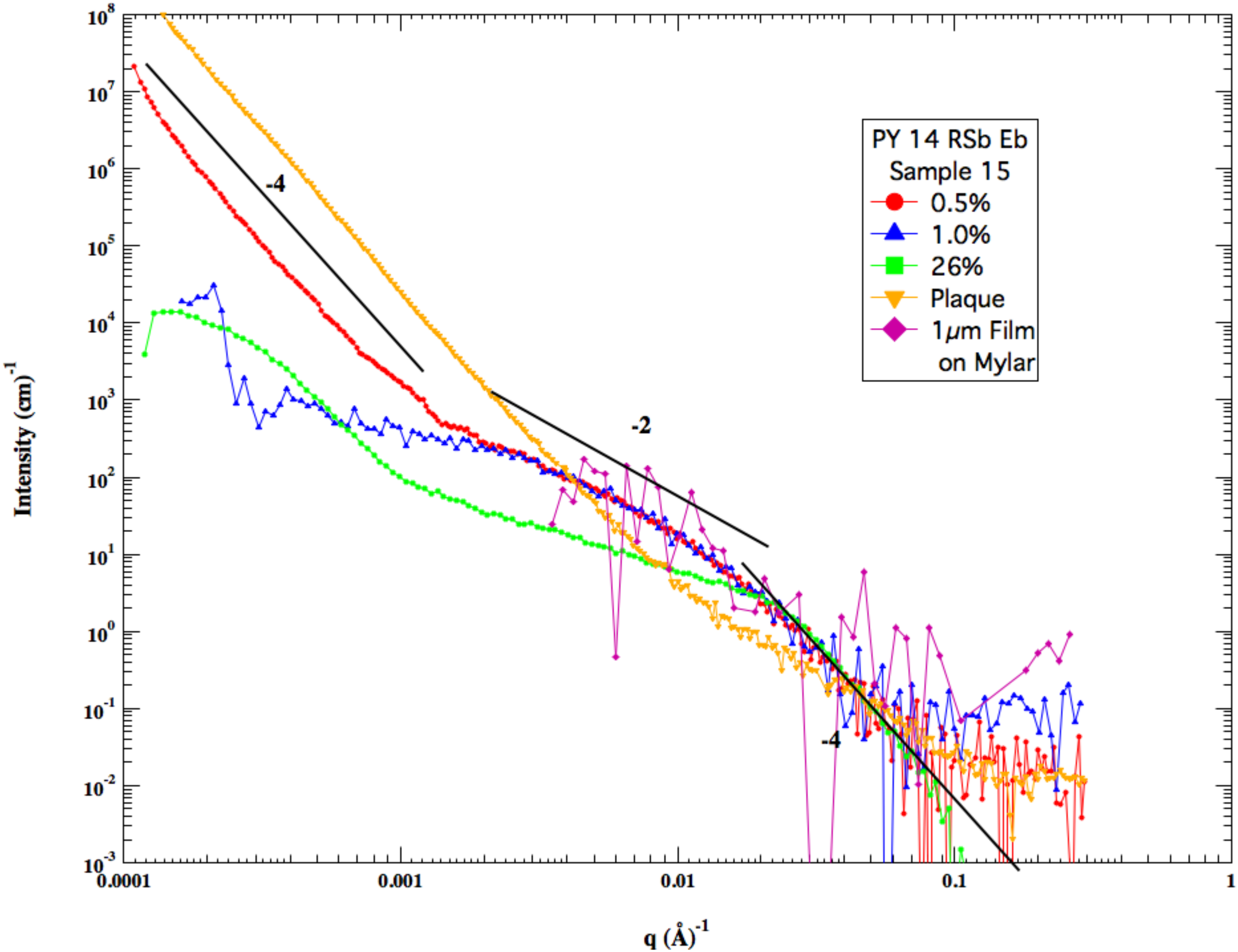

PY 14 RSb Eb
Sample 15
0.5%
1.0%
26%
Plaque
1μm Film
on Mylar
-4
-2
-4
Intensity (cm)$^{-1}$
q (Å)$^{-1}$
10^{8}
10^{7}
10^{6}
10^{5}
10^{4}
10^{3}
10^{2}
10^{1}
10^{0}
10^{-1}
10^{-2}
10^{-3}
0.0001
0.001
0.01
0.1
1

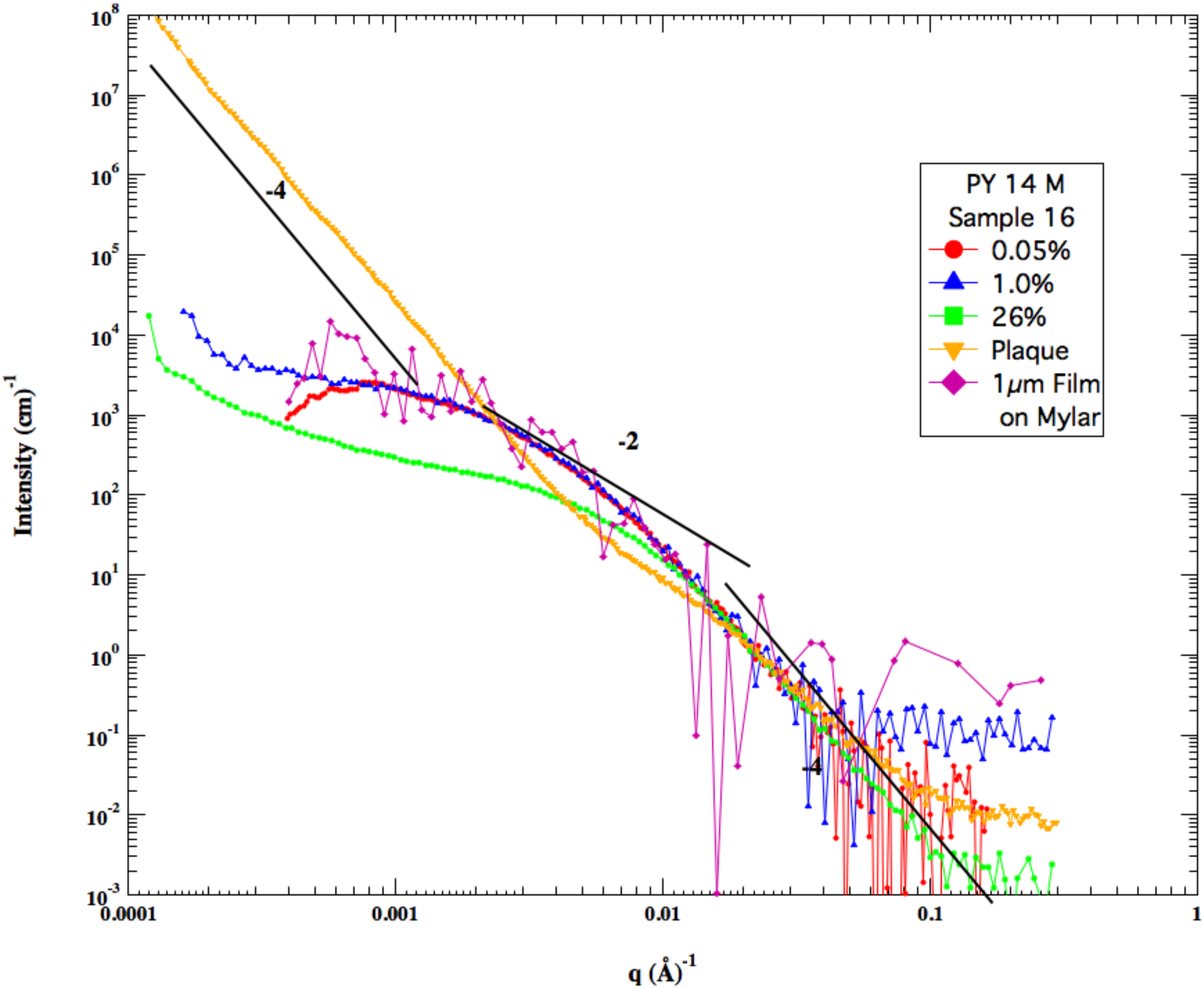

PY 14 M
Sample 16
0.05%
1.0%
26%
Plaque
1μm Film
on Mylar
-4
-2
-4
Intensity (cm)$^{-1}$
q (Å)$^{-1}$

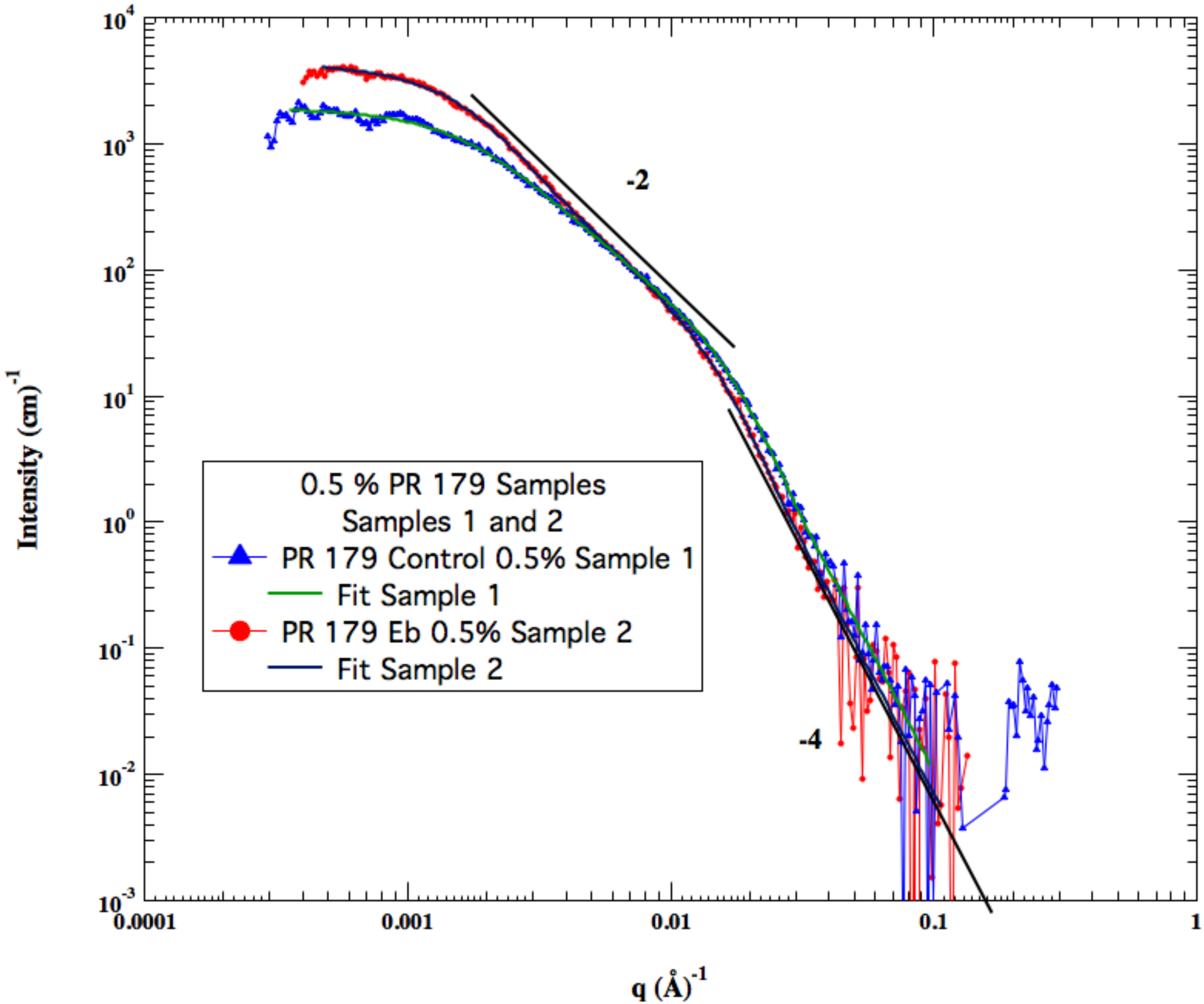

0.5 % PR 179 Samples
Samples 1 and 2
PR 179 Control 0.5% Sample 1
Fit Sample 1
PR 179 Eb 0.5% Sample 2
Fit Sample 2
-2
-4
Intensity (cm)^-1
q (Å)^-1
0.0001
0.001
0.01
0.1
1

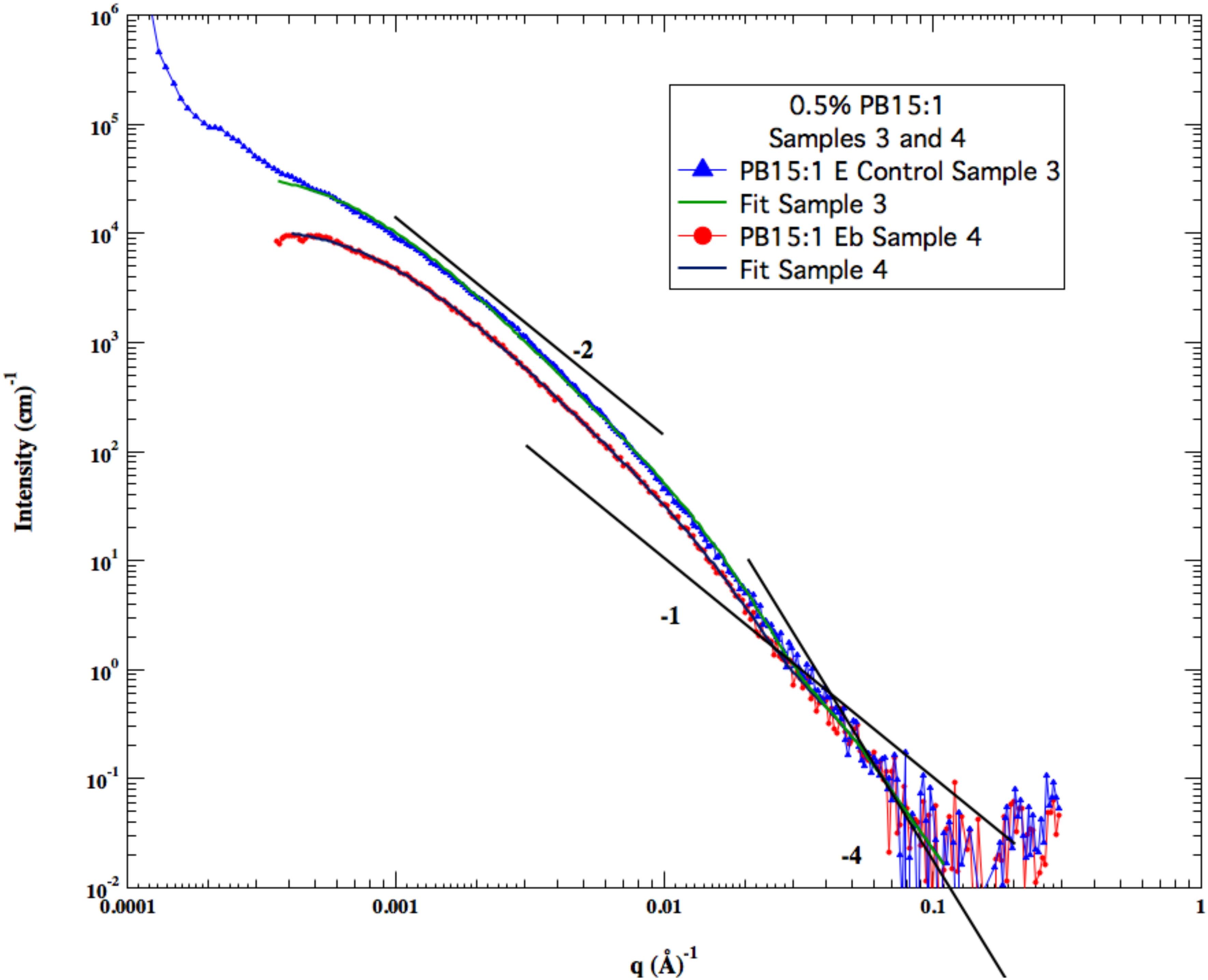

0.5% PB15:1
Samples 3 and 4
PB15:1 E Control Sample 3
Fit Sample 3
PB15:1 Eb Sample 4
Fit Sample 4
-2
-1
-4
Intensity (cm)-1
q (Å)-1
0.0001
0.001
0.01
0.1
1

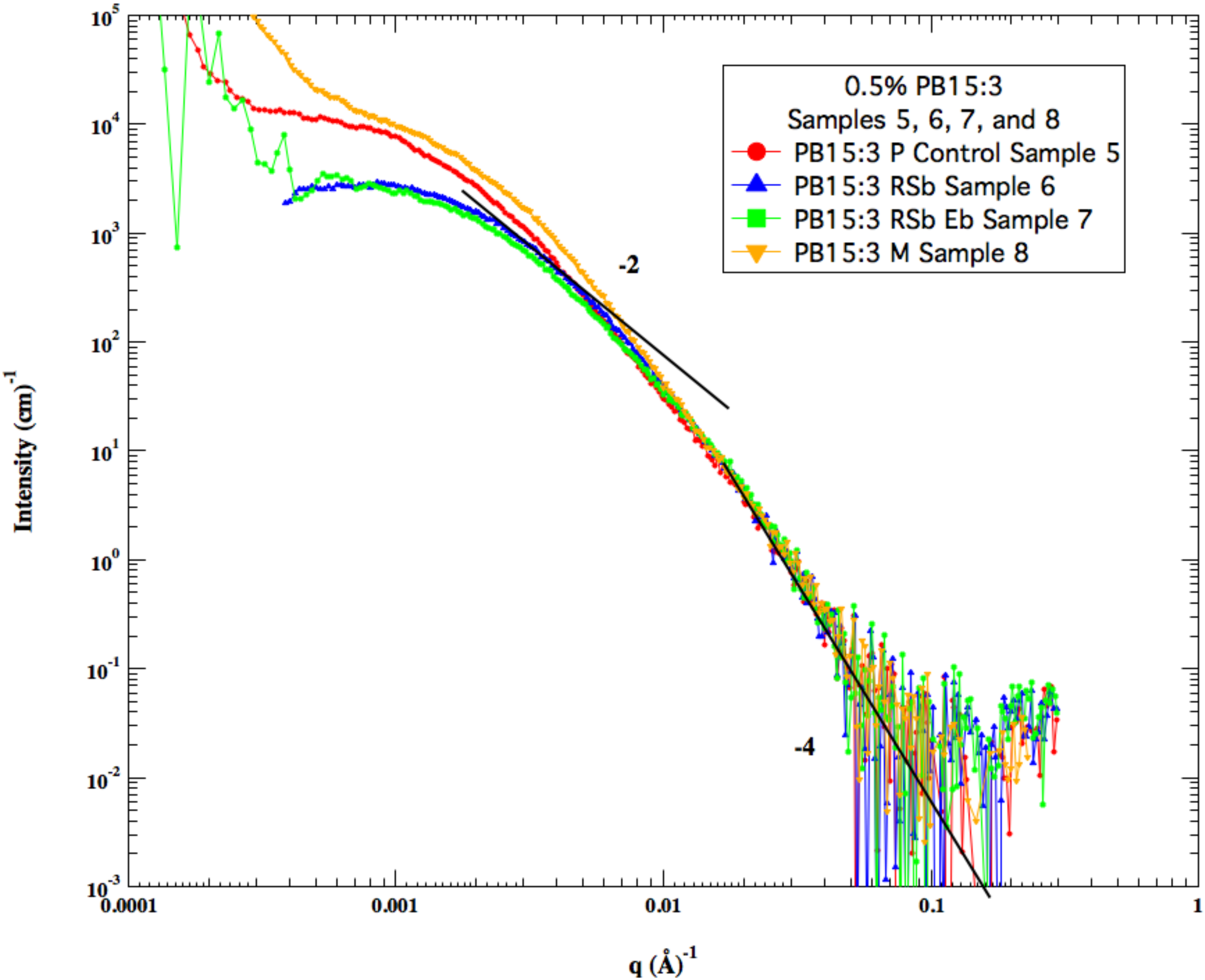
0.5% PB15:3
Samples 5, 6, 7, and 8
PB15:3 P Control Sample 5
PB15:3 RSb Sample 6
PB15:3 RSb Eb Sample 7
PB15:3 M Sample 8
-2
-4
Intensity (cm)-1
q (Å)-1
0.0001
0.001
0.01
0.1
1
10^5
10^4
10^3
10^2
10^1
10^0
10^-1
10^-2
10^-3

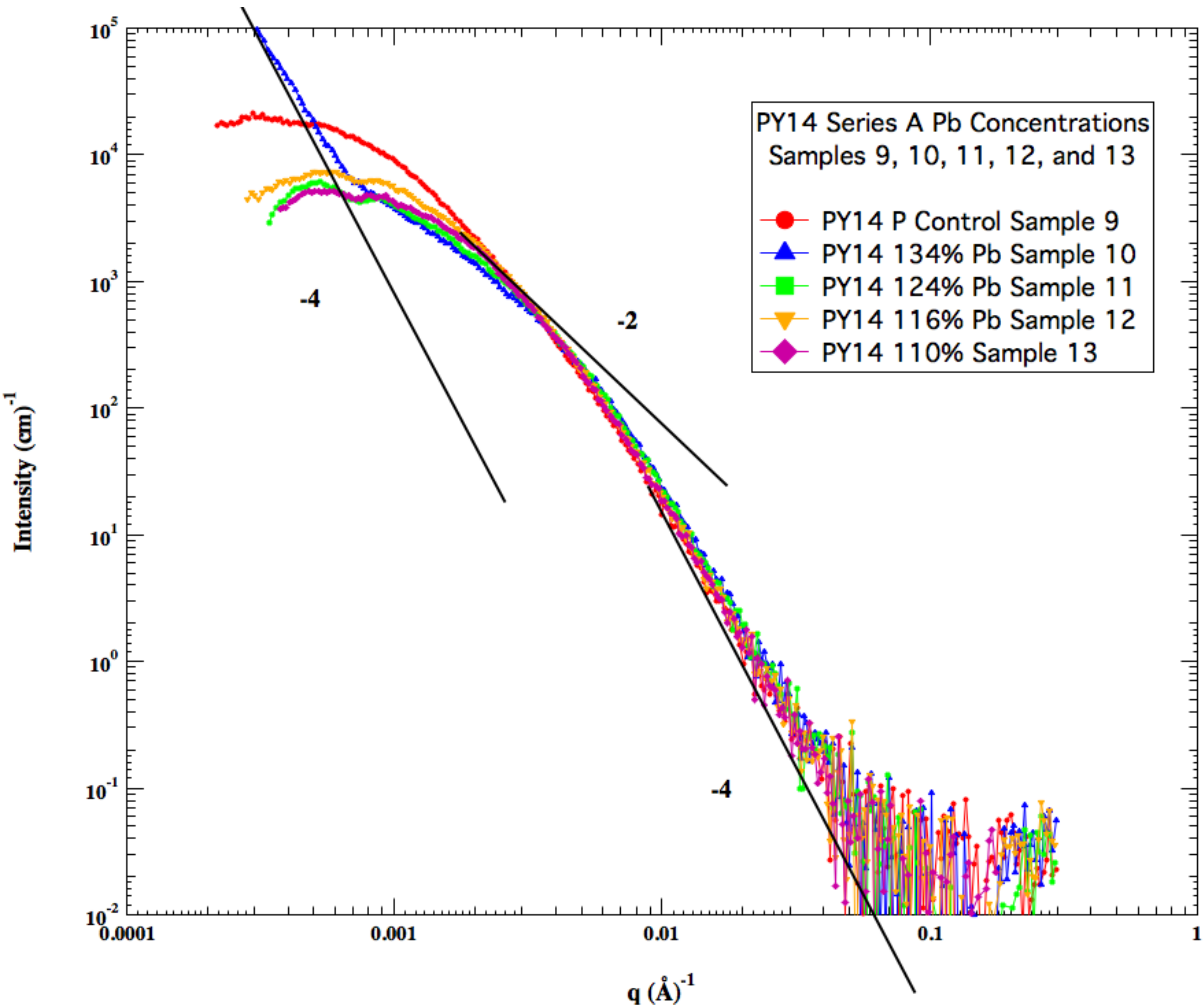

PY14 Series A Pb Concentrations
Samples 9, 10, 11, 12, and 13
PY14 P Control Sample 9
PY14 134% Pb Sample 10
PY14 124% Pb Sample 11
PY14 116% Pb Sample 12
PY14 110% Sample 13
-4
-2
-4
Intensity (cm)-1
q (Å)-1
10^5
10^4
10^3
10^2
10^1
10^0
10^-1
10^-2
0.0001
0.001
0.01
0.1
1

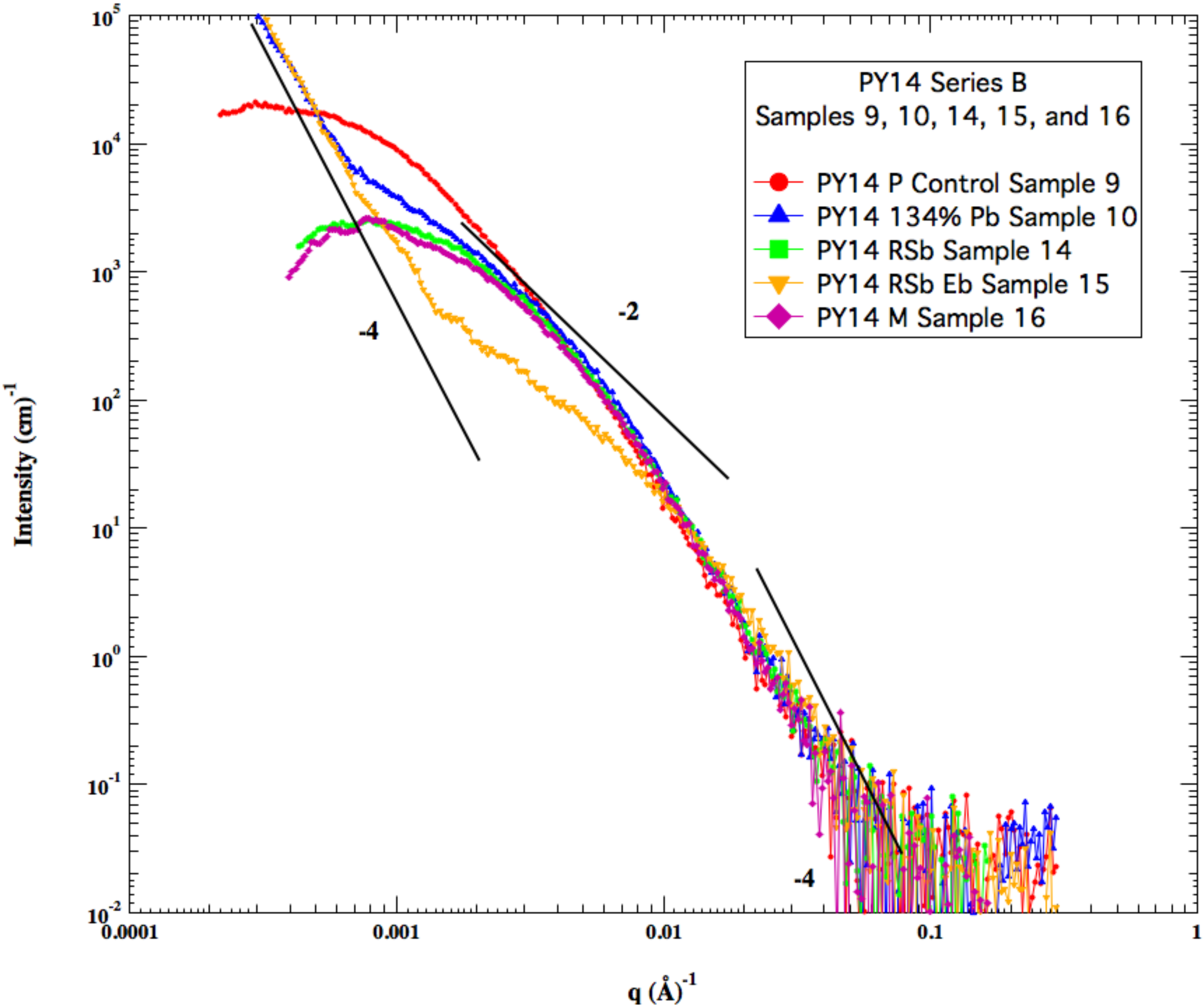
PY14 Series B
Samples 9, 10, 14, 15, and 16
PY14 P Control Sample 9
PY14 134% Pb Sample 10
PY14 RSb Sample 14
PY14 RSb Eb Sample 15
PY14 M Sample 16
-4
-2
-4
Intensity (cm)$^{-1}$
q (Å)$^{-1}$
10^5
10^4
10^3
10^2
10^1
10^0
10^{-1}
10^{-2}
0.0001
0.001
0.01
0.1
1

Summary

1) 16x5 Samples Run
   80 Samples (+ 8 Dilutions)

2) 0.05% Samples fit and tabulated
   16 Samples

3) Generally concentration series qualitatively follow the RPA formulation
   In some cases it didn't, e.g. PB15:1

4) Generally 1μm Films on Mylar showed enhanced aggregation
   In some cases they didn't, specifically the PY14 samples except Py14 RSb

5) More analysis is needed but this will take several weeks

Scaling Model

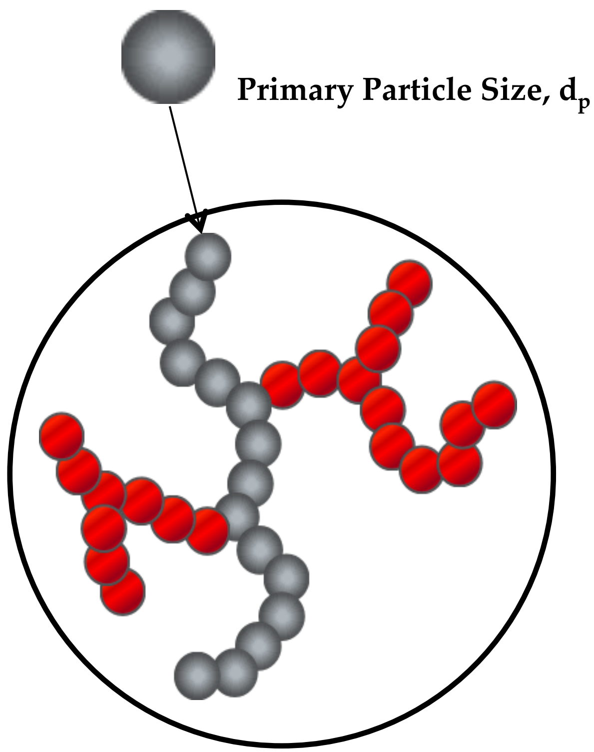

z **Primary Particles, Dimension** d_f **,**
Size d_p

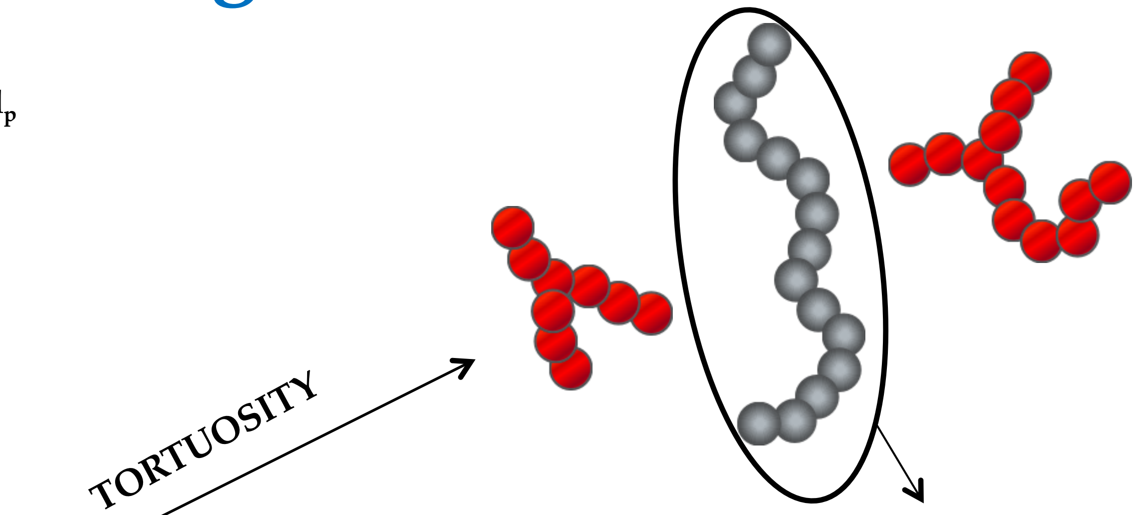

Minimum path p **: dimension** d_{min}

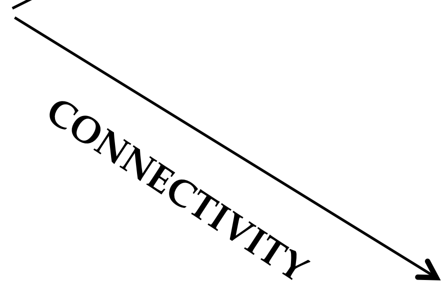

$$z \sim \left(\frac{R}{l_k}\right)^{d_f} ; p \sim \left(\frac{R}{l_k}\right)^{d_{\min}} ; s \sim \left(\frac{R}{l_k}\right)^{c}$$

$$z \sim p^c \sim s^{d_{\min}}$$
$$d_f = c d_{\min}$$

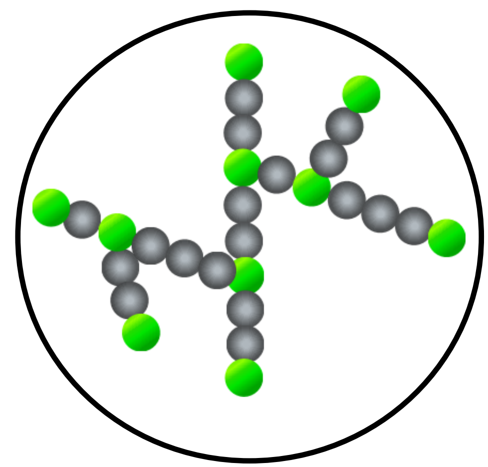

Connective path s **: dimension** c

Beaucage, G., Determination of branch fraction and minimum dimension of mass-fractal aggregates. *Physical Review E* **2004,** *70* (3).

SANS From Persistent Chains

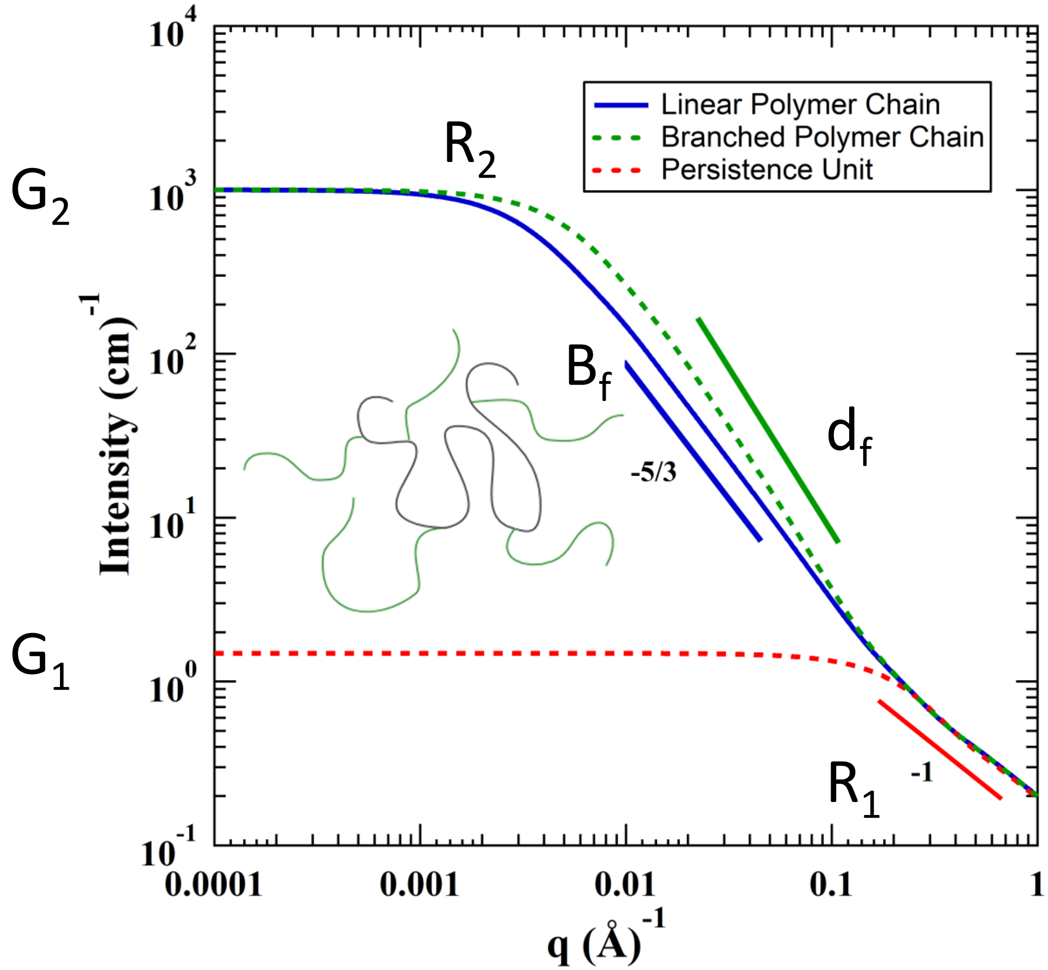

$$d_{min} = \frac{B_f R_{g,2}^{d_f}}{G_2 \Gamma\left(d_f/2\right)}$$

Beaucage, G., Determination of branch fraction and minimum dimension of mass-fractal aggregates. *Physical Review E* **2004,** *70* (3).

Guinier's Law	Power Law	Scattering Vector
$I(q) = G \exp\left(\frac{-q^2 R_g^2}{3}\right)$	$I(q) = B_f q^{-d_f}$	$q = \frac{4\pi}{\lambda}\sin\left(\frac{\theta}{2}\right)$

Quantification of Branching

Mole-Fraction LCB Content

$$\phi_{br} = \frac{z-p}{z} = 1 - z^{\frac{1}{c}-1}$$

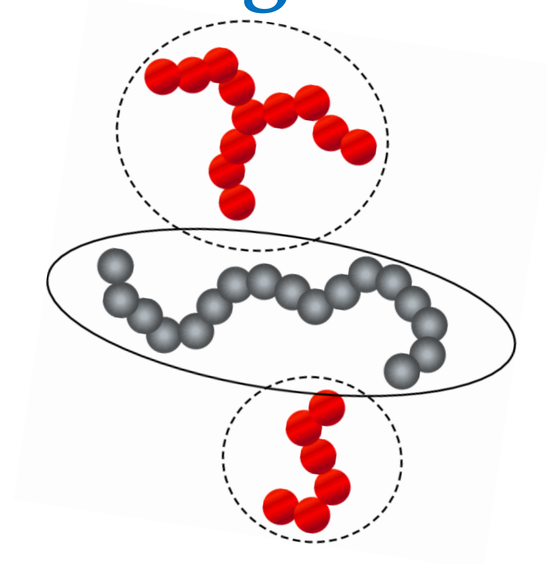

Average number of branch points per chain

$$n_{br} = \left(\frac{z^{\left(\frac{5}{2d_f} - \frac{3}{2c}\right) + \left(1 - \frac{1}{c}\right)} - 1}{2} \right)$$

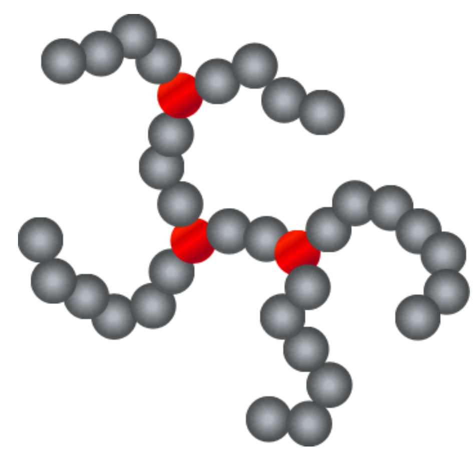

•Beaucage, G., Determination of branch fraction and minimum dimension of mass-fractal aggregates. *Physical Review E* **2004,** *70* (3).
•Ramachandran, R.; Beaucage, G.; Kulkarni, A. S.; McFaddin, D.; Merrick-Mack, J.; Galiatsatos, V., Branch Content of Metallocene Polyethylene. *Macromolecules* **2009,** *42* (13), 4746-4750.

Quantification of Branching

Mole-Fraction LCB Content

$$\phi_{br} = \frac{z-p}{z} = 1 - z^{\frac{1}{c}-1}$$

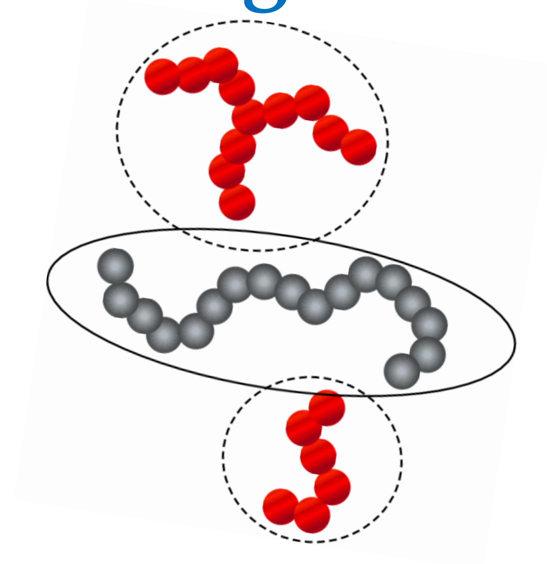

Average number of branch points per chain

$$n_{br} = \left(\frac{z^{\left(\frac{5}{2d_f} - \frac{3}{2c}\right) + \left(1 - \frac{1}{c}\right)} - 1}{2} \right)$$

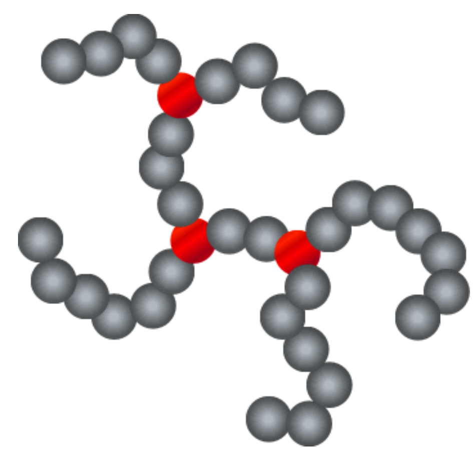

•Beaucage, G., Determination of branch fraction and minimum dimension of mass-fractal aggregates. *Physical Review E* **2004,** *70* (3).
•Ramachandran, R.; Beaucage, G.; Kulkarni, A. S.; McFaddin, D.; Merrick-Mack, J.; Galiatsatos, V., Branch Content of Metallocene Polyethylene. *Macromolecules* **2009,** *42* (13), 4746-4750.

Quantification of Branching

Average LCB length

$$z_{br} = \frac{z\phi_{br}M_{Kuhn}}{n_{br(NMR\ or\ SANS)}}$$

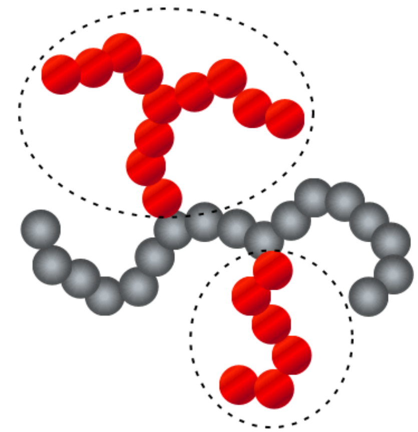

Hyperbranch Content (Branch-on-Branch)

$$n_i = n_{br} - n_{br,p}$$

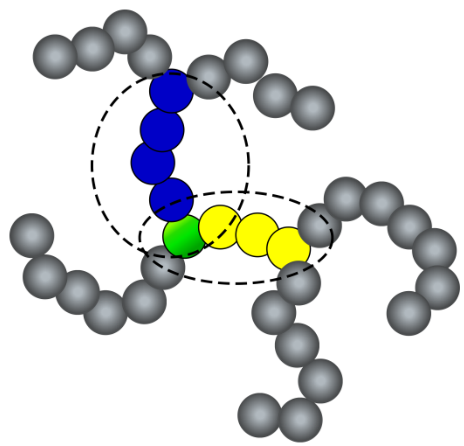

•Beaucage, G., Determination of branch fraction and minimum dimension of mass-fractal aggregates. *Physical Review E* **2004,** *70* (3).
•Ramachandran, R.; Beaucage, G.; Kulkarni, A. S.; McFaddin, D.; Merrick-Mack, J.; Galiatsatos, V., Branch Content of Metallocene Polyethylene. *Macromolecules* **2009,** *42* (13), 4746-4750.

Literature Data, Dreiss (2007)

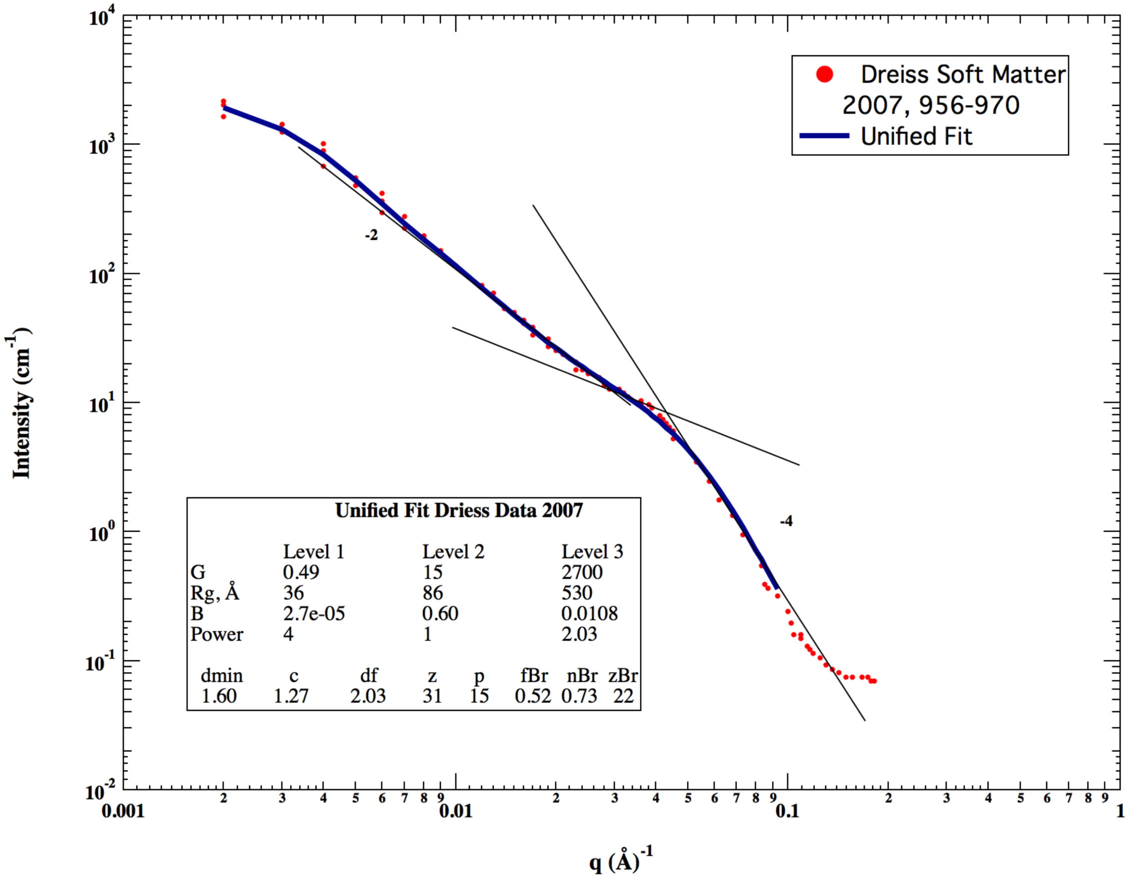

Figure 3. SANS data from Dreiss from branched worm-like micelles (WLMs). Data is fit to the unified function and analyzed using the scaling-model. G is I(0), B the power-law prefactor, fBr is the mole fraction branches in the structure, n_{Br} is the number of branches per chain, z_{Br} the average branch length. Other parameters are described in the text. The data shows that the WLMs display persistence and self-avoiding walk scaling ($d_{min} \sim 1.67$). The analysis indicates that 3 of 4 WLM chains are branched, the chains are composed of 180 Kuhn units on average with an average branch length of 128 Kuhn units. The average short circuit path through these structures is 87 Kuhn units. The Kuhn length is about 30 nm. The diameter of the micelle is about 8.3 nm. The contour length of the micelle is about 0.9 µm.

$l_p = \sqrt{3}R_{g,2} = 14.9$ nm
$R = 4\, R_{g,1}/\sqrt{3} = 8.3$ nm
$\phi_{Br} = 0.52$
$n_{Br} = 0.7$
$z_{Br} = 22$
$z = 180$
$L = 0.9$ µm

Work of Nikhil Agashe *C. I. Pigment Yellow 14*

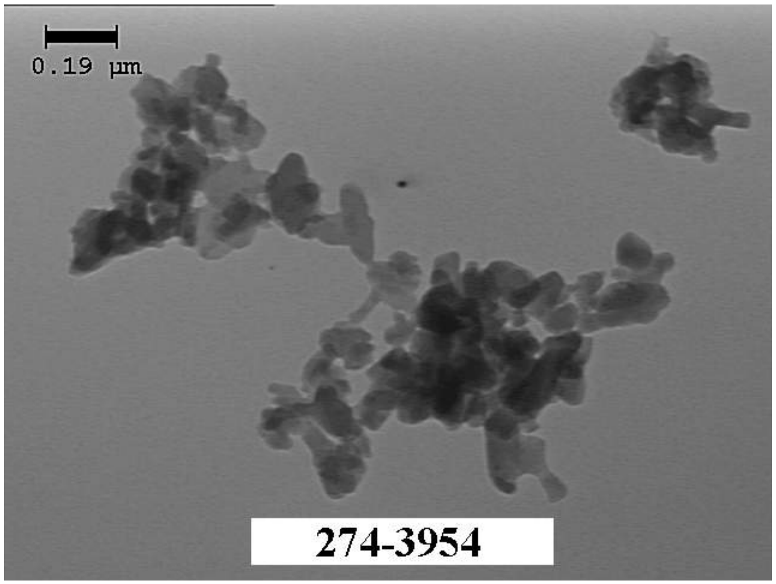

C. I. PY 14

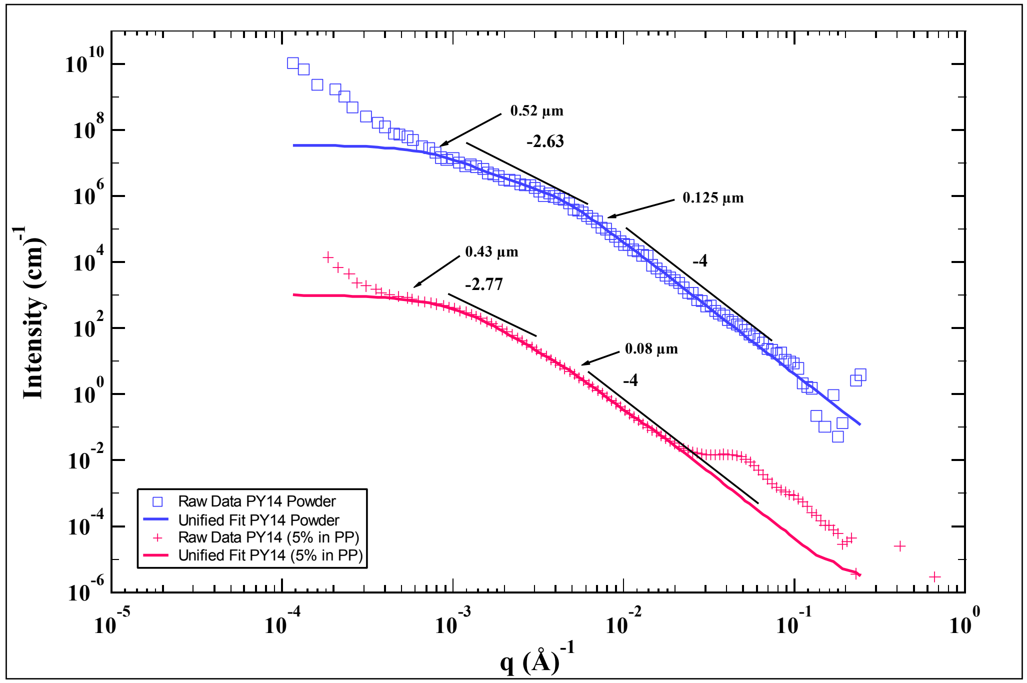

Sample	m_{Porod}	d_f	Rg_1 (µm)	Rg_2 (µm)	G_1	G_2
Powder	-4	2.63±0.04	0.048	0.1995	34065	4.12e05
5% in PP	-4	2.77±0.02	0.031	0.1662	534.85	1.72e05

Table 7.03 SAXS Data for C. I. PY 14 (**m_{Porod}**: power law slope of scattering curve in Porod regime, **d_f**: fractal dimension, **Rg**: radius of gyration, **G**: Guinier prefactor)

Work of Nikhil Agashe *C. I. Pigment Yellow 14*

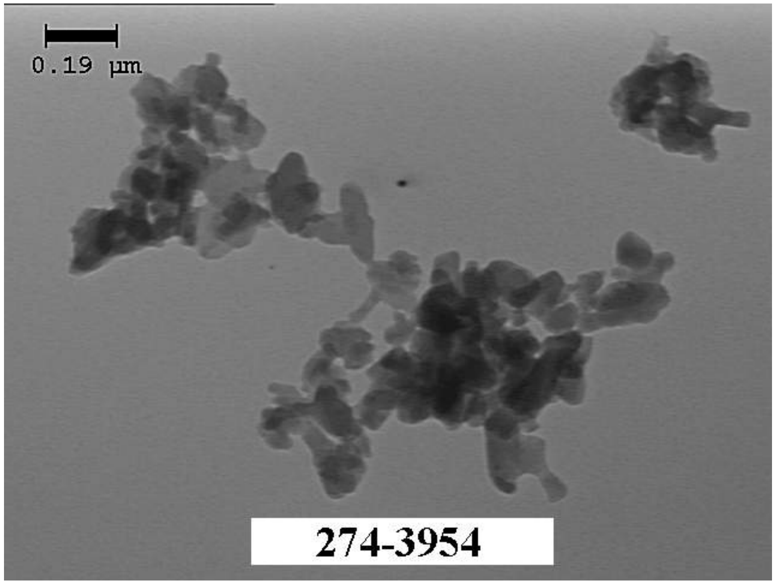

C. I. PY 14

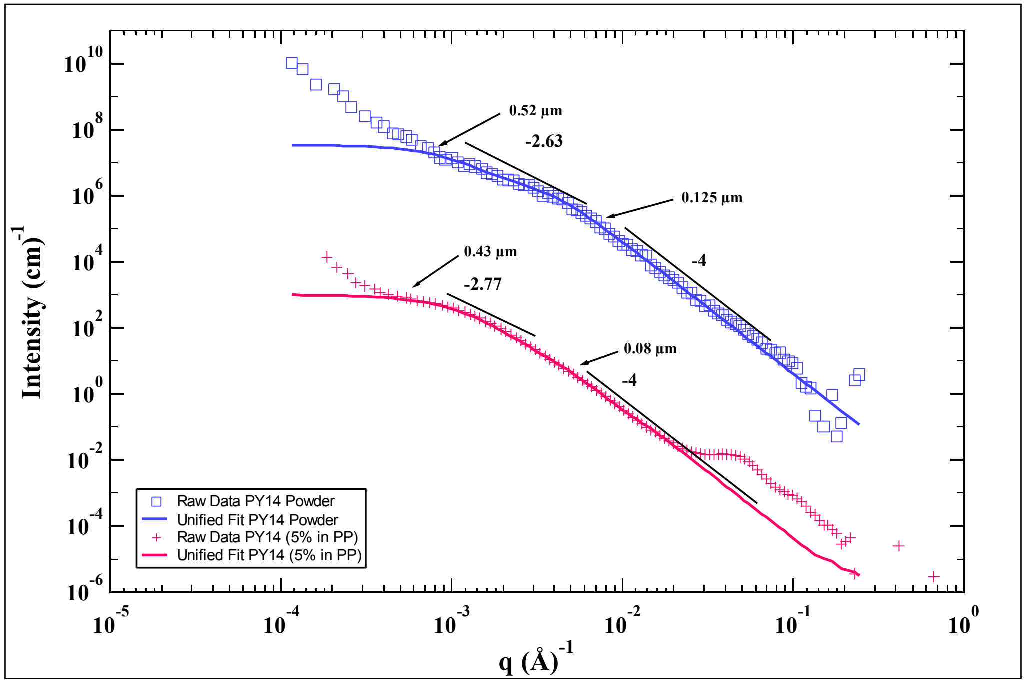

Value	**D**primary **(µm)**	**D**aggregate **(µm)**	**DOA**$_1$	**DOA**$_2$
Powder	0.125	0.52	12	23
5% in PP	0.08	0.43	321	42

Table 7.04 SAXS calculations for PY 14 (**D**$_{primary}$: calculated size of the primary particle based on diameter of an equivalent sphere, **D**$_{aggregate}$: calculated size of the aggregate based on diameter of an equivalent sphere, **DOA**: degree of aggregation)

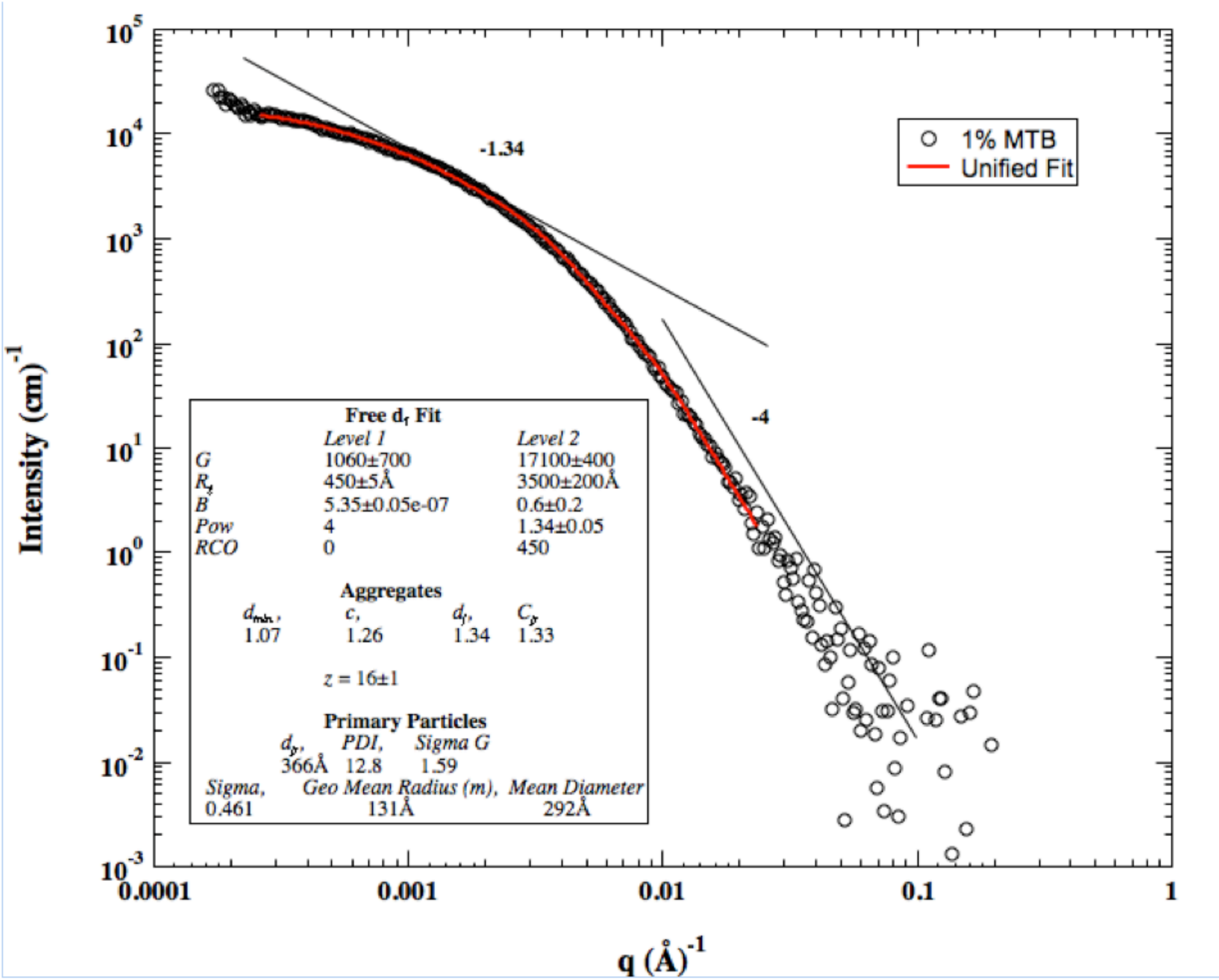

Figure 1. USAXS data from 1% aqueous suspension of MTB pigment YFD 1123 (Yellow 14).

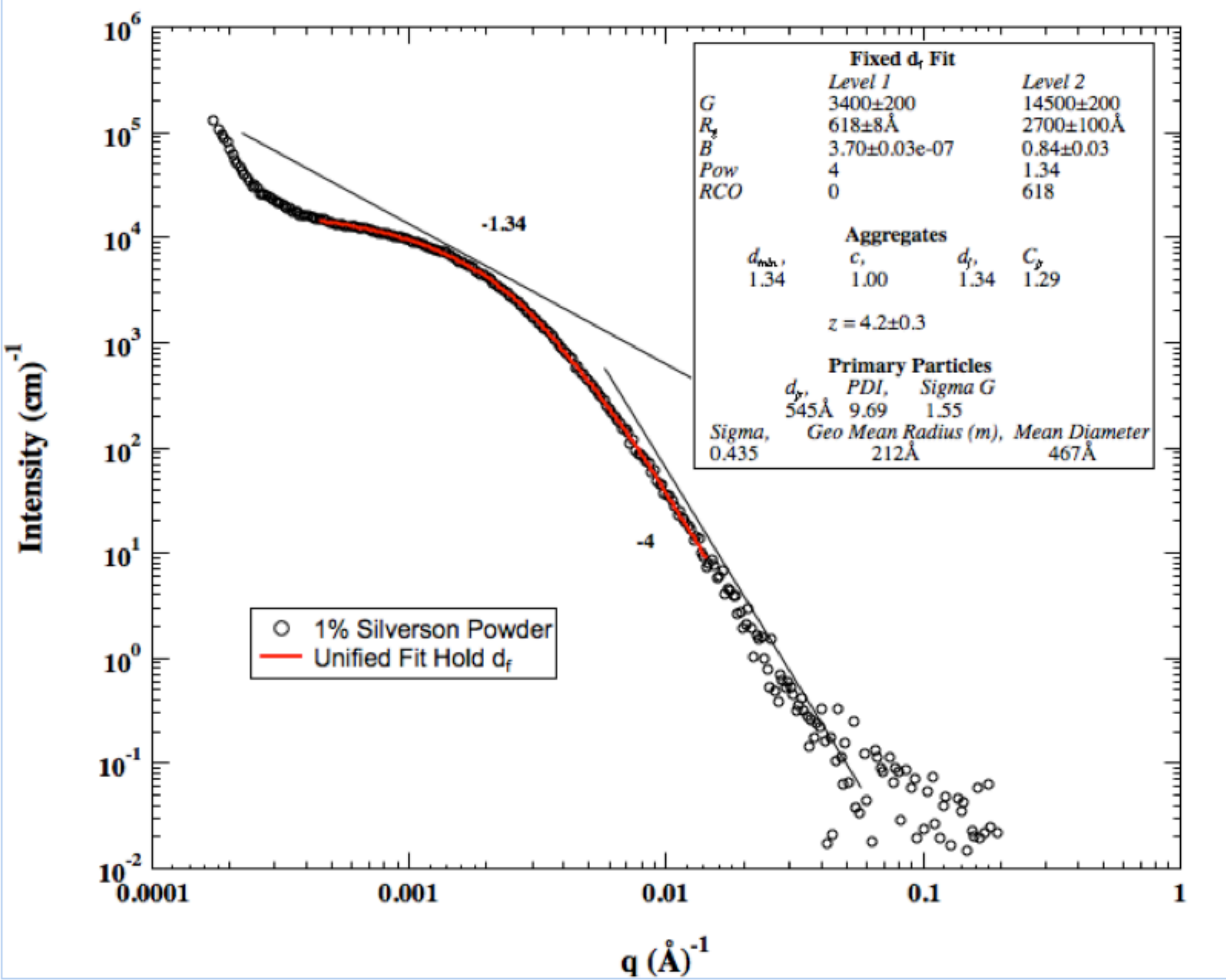

Figure 2. USAXS data from 1% aqueous suspension of Silverson milled pigment YFD 1123 (Yellow 14).

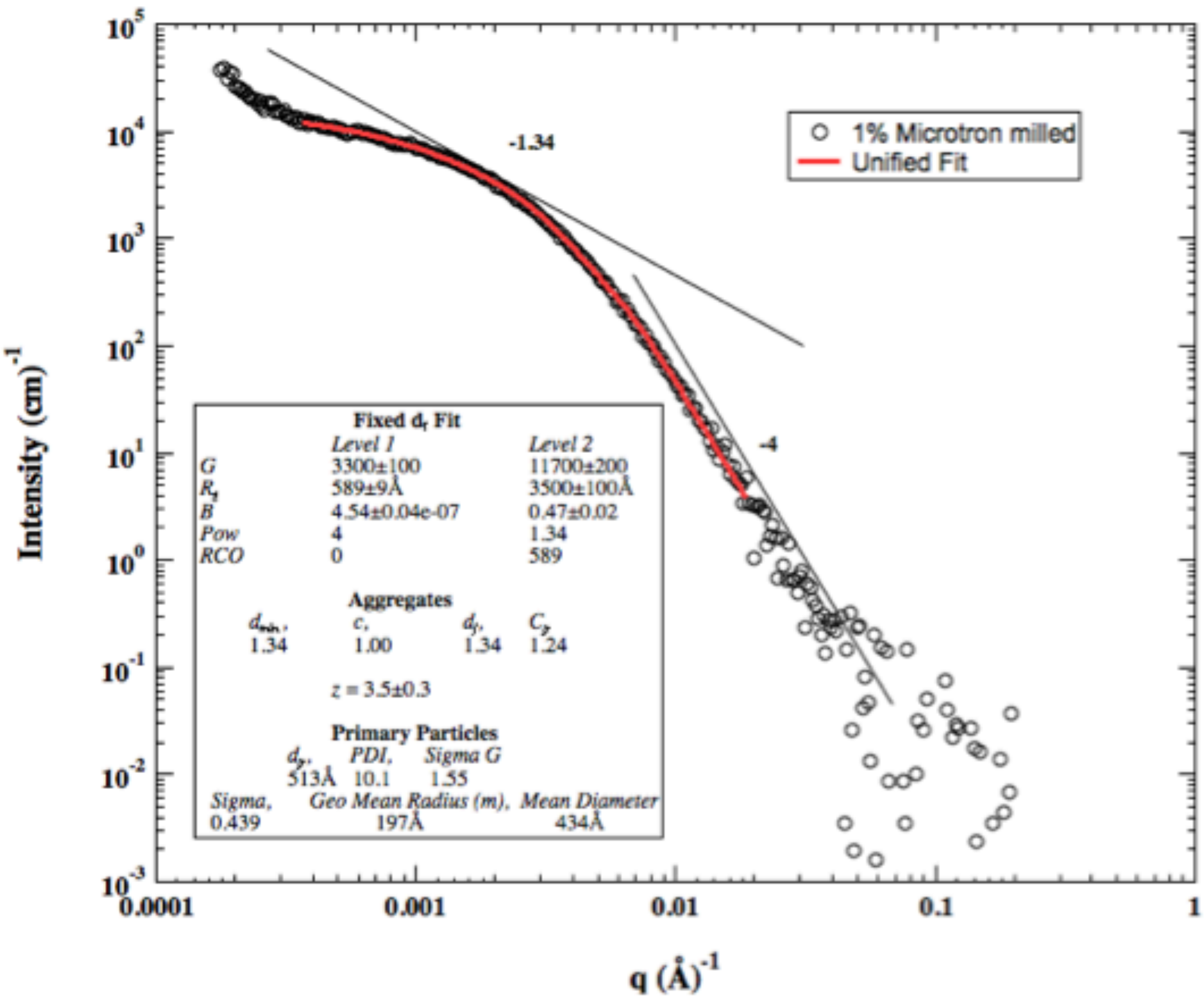

Figure 3. USAXS data from 1% aqueous suspension of Microtron milled pigment YFD 1123 (Yellow 14).

Table 2. Fit results for one weight percent aqueous dispersions.

	R_{g1}, Å	d_p, Å	σ_g	R_{g2}, Å	C_p	z	d_f	$V_{sp}/V_{0,sp}$	χ
MTB	450±5	366	1.59	3500±200	1.33	16±1	1.34	7.00	0.33
Microtron	589±9	513	1.55	3500±100	1.24	3.5±0.3	(*1.34*)	13.6	0.12
Silverson	618±8	545	1.55	2700±100	1.29	4.2±0.3	(*1.34*)	9.30	0.27

Concentration Series

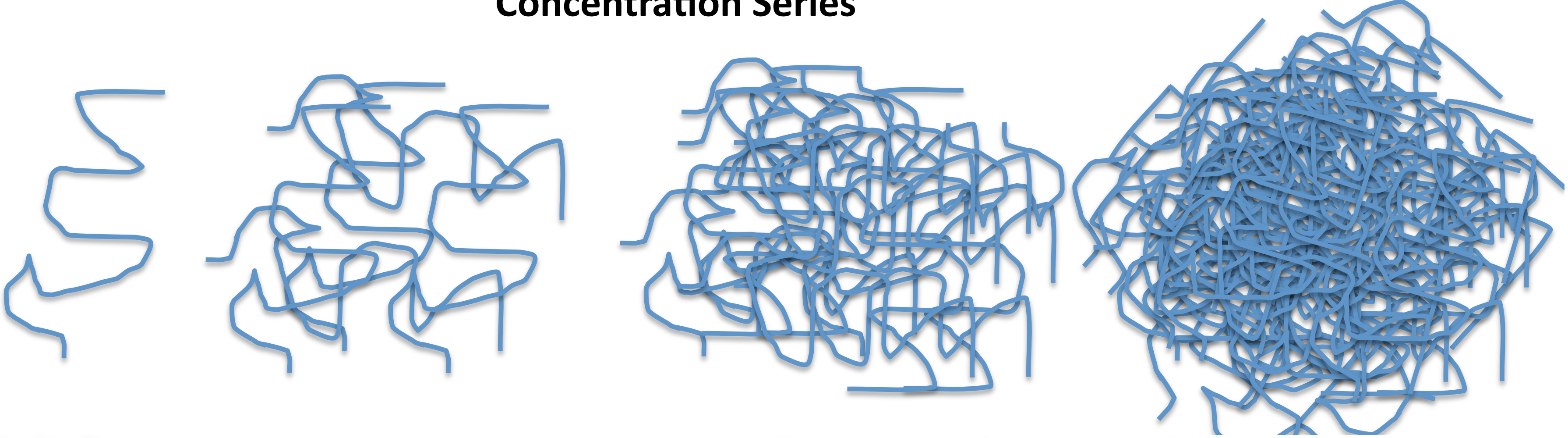

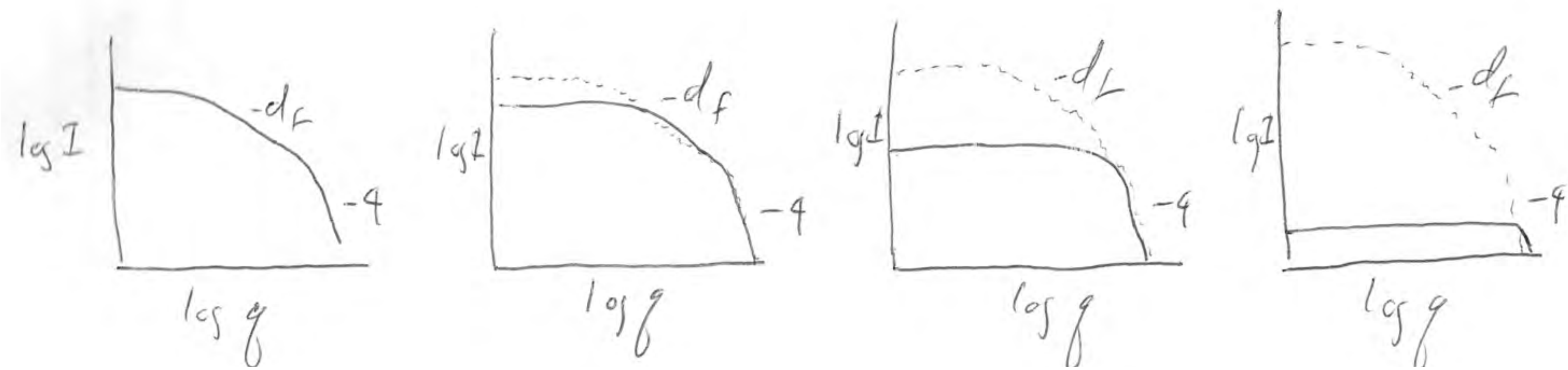

$$1/I(q, \Phi_V) = 1/I(q, \Phi_V{=}0) + \Phi_V\,(V_{sp}/V_{0,sp})\,(1/(1 - \Phi_V) - 2\chi)/I(q{=}0, \Phi_V{=}0) \tag{3}$$

where χ is an enthalpic interaction between solvent and a subunit of the aggregate, and $(V_{sp}/V_{0,sp})$ is the ratio of the volume of that subunit and the volume of a water molecule. In this case, the subunit is ill defined and we could just consider the more generic second virial coefficient,

$$2A_2 = (1/(1 - \Phi_V) - 2\chi) \tag{4}.$$

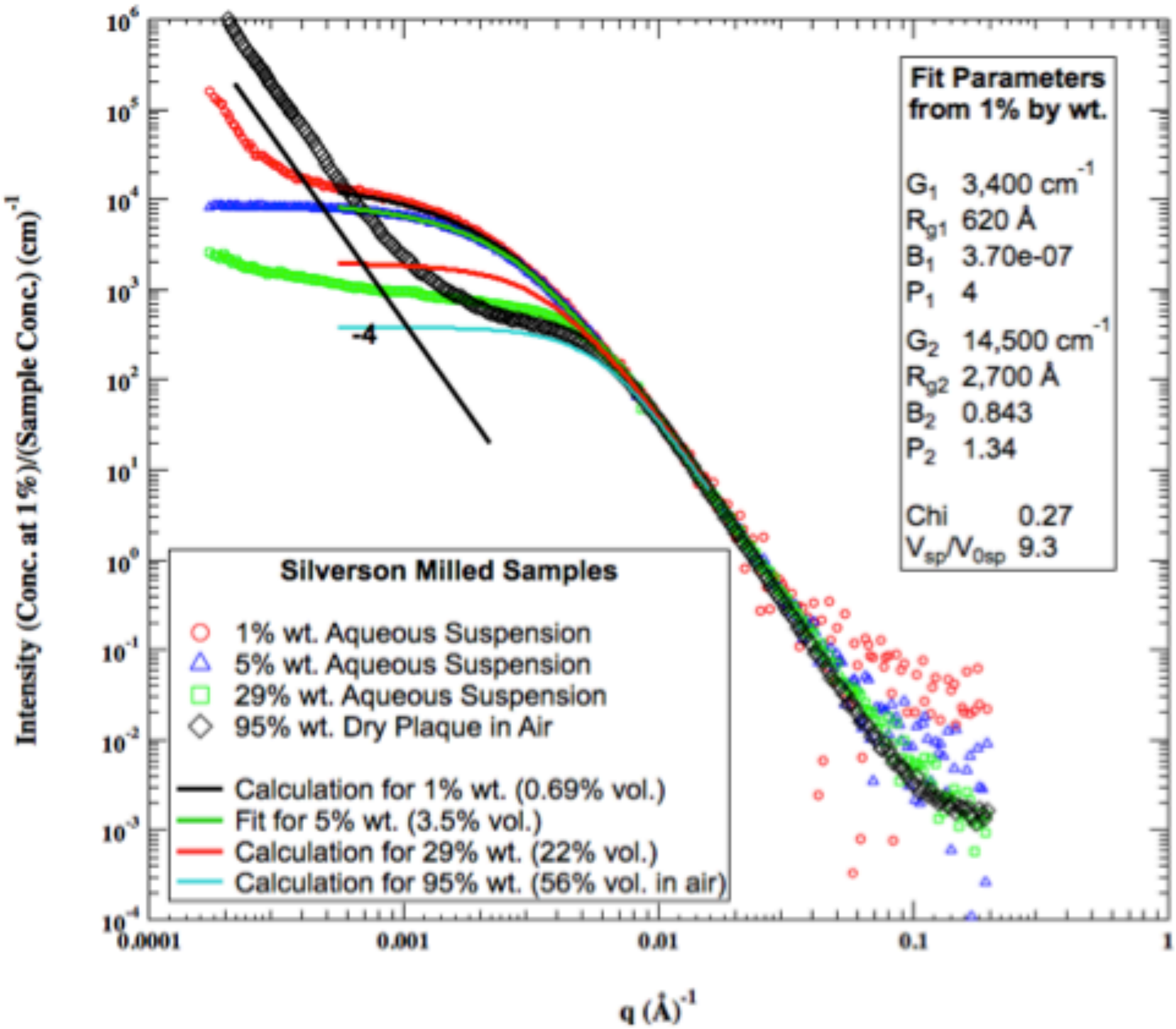

Figure 4. USAXS data from aqueous suspensions and dry plaque of Silverson milled pigment YFD 1123 (Yellow 14) with RPA fit (Equation (3)) to five weight percent sample and calculations based on this fit for one, 29 and 95 weight percentages. Chi and the volume ratio are fit for the 5% by weight curve (shown in inset) and all other curves are calculated based on the volume fraction. The other calculation parameters come from the fit to the one weight percent sample in Figure 1.

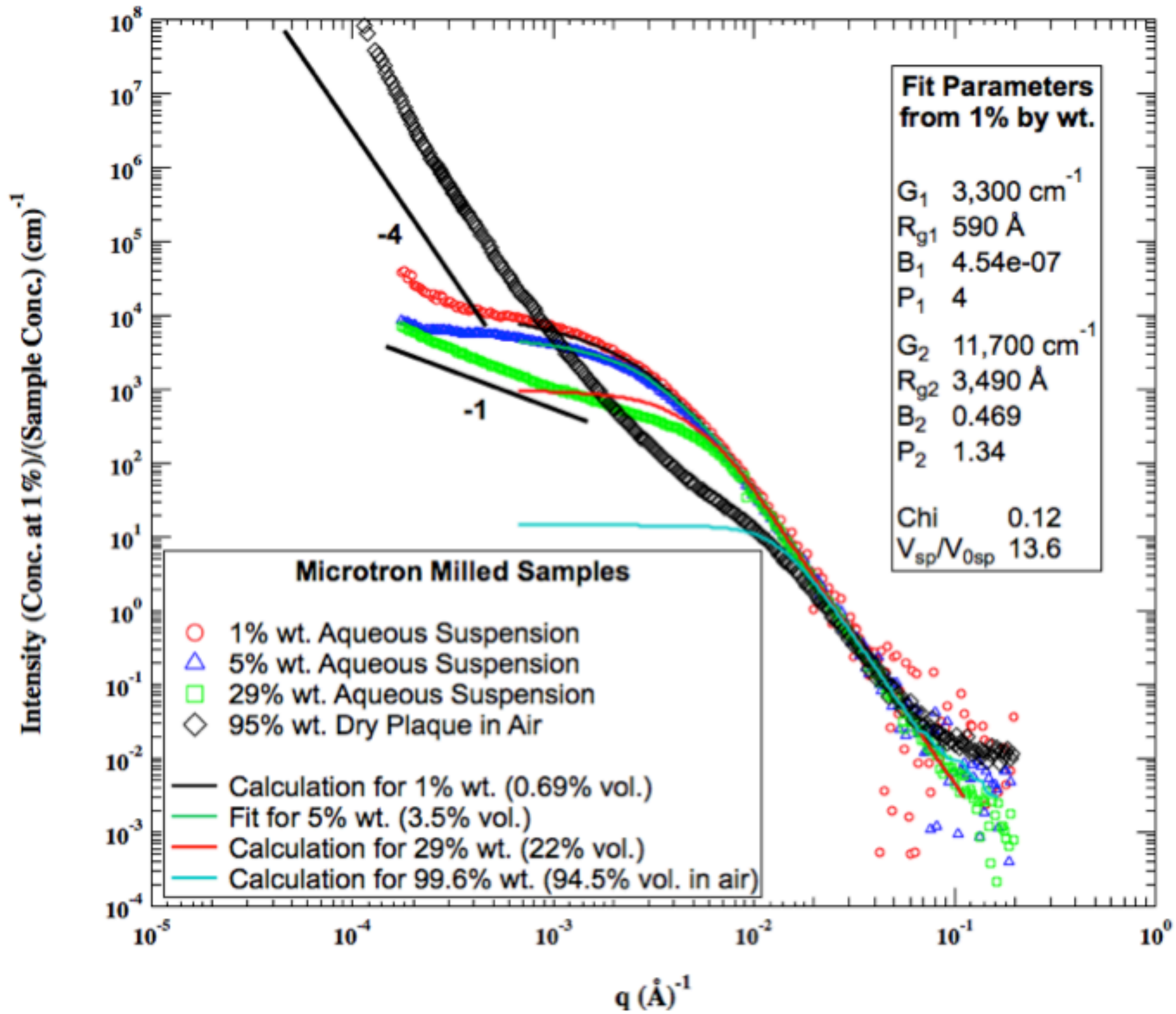

Figure 5. USAXS data from aqueous suspensions and dry plaque of Microtron milled pigment YFD 1123 (Yellow 14) with RPA fit (Equation (3)) to five weight percent sample and calculations based on this fit for one, 29 and 95 weight percentages. Chi and the volume ratio are fit for the 5% by weight curve (shown in inset) and all other curves are calculated based on the volume fraction. The other calculation parameters come from the fit to the one weight percent sample in Figure 2.

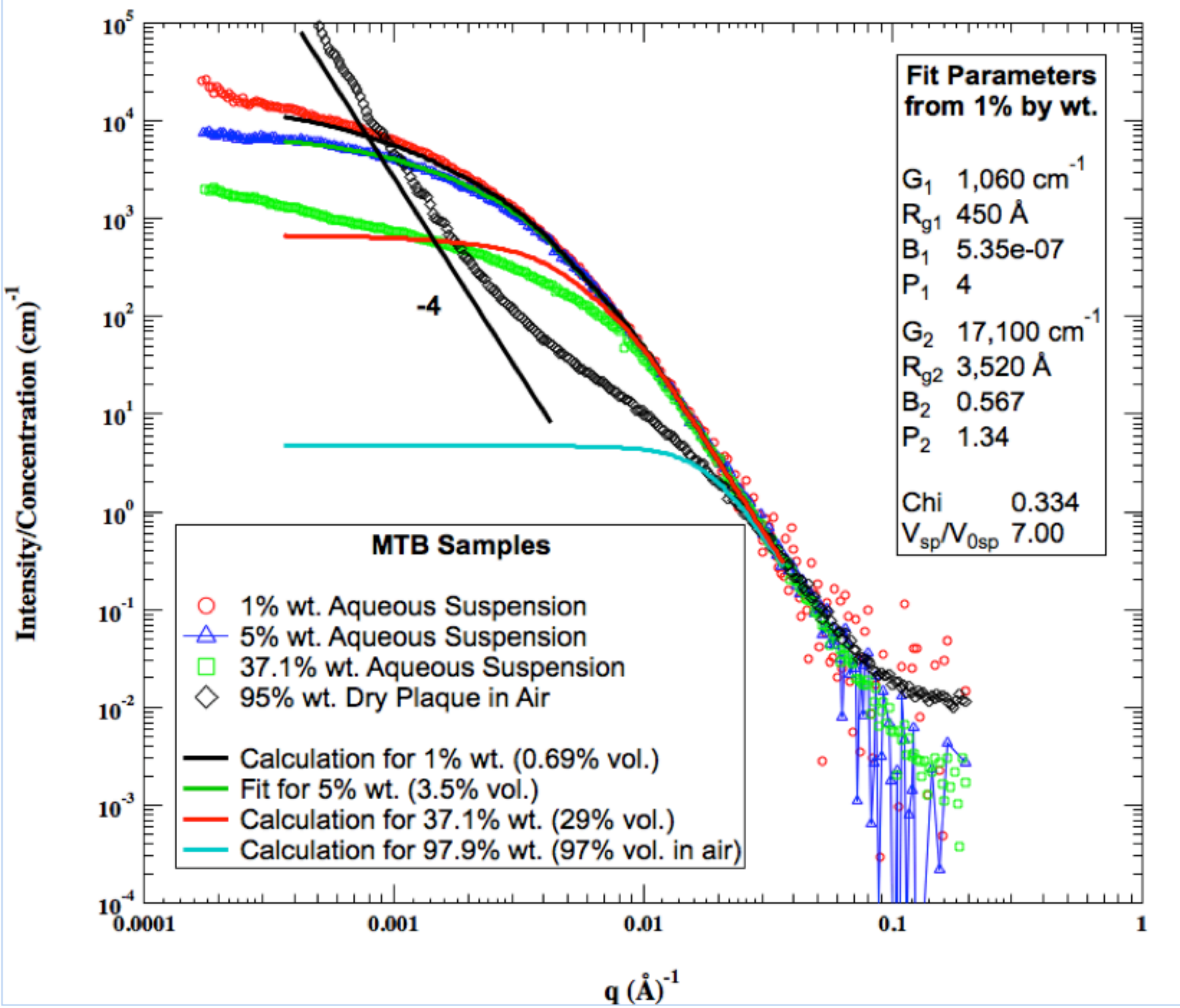

Figure 6. USAXS data from aqueous suspensions and dry plaque of MTB powder pigment YFD 1123 (Yellow 14) with RPA fit (Equation (3)) to five weight percent sample and calculations based on this fit for one, 29 and 95 weight percentages. Chi and the volume ratio are fit for the 5% by weight curve (shown in inset) and all other curves are calculated based on the volume fraction. The other calculation parameters come from the fit to the one weight percent sample in Figure 3.

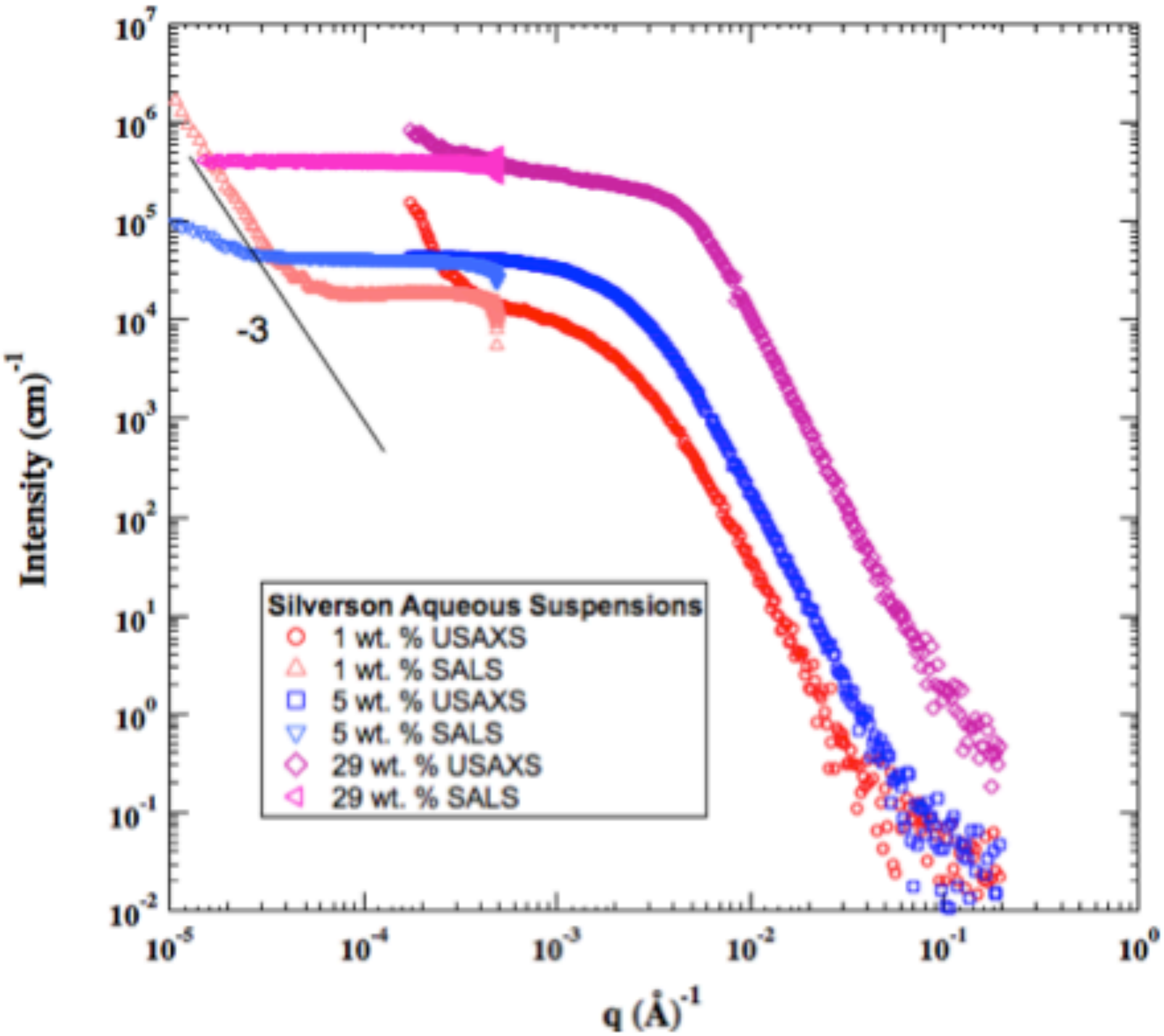

Figure 7. SALS and USAXS data from aqueous suspensions of Silverson milled pigment YFD 1123 (Yellow 14). Data for the one weight percent and 29 weight percent samples do not agree with USAXS data due to contrast differences and multiple scattering for the 29 weight percent sample.

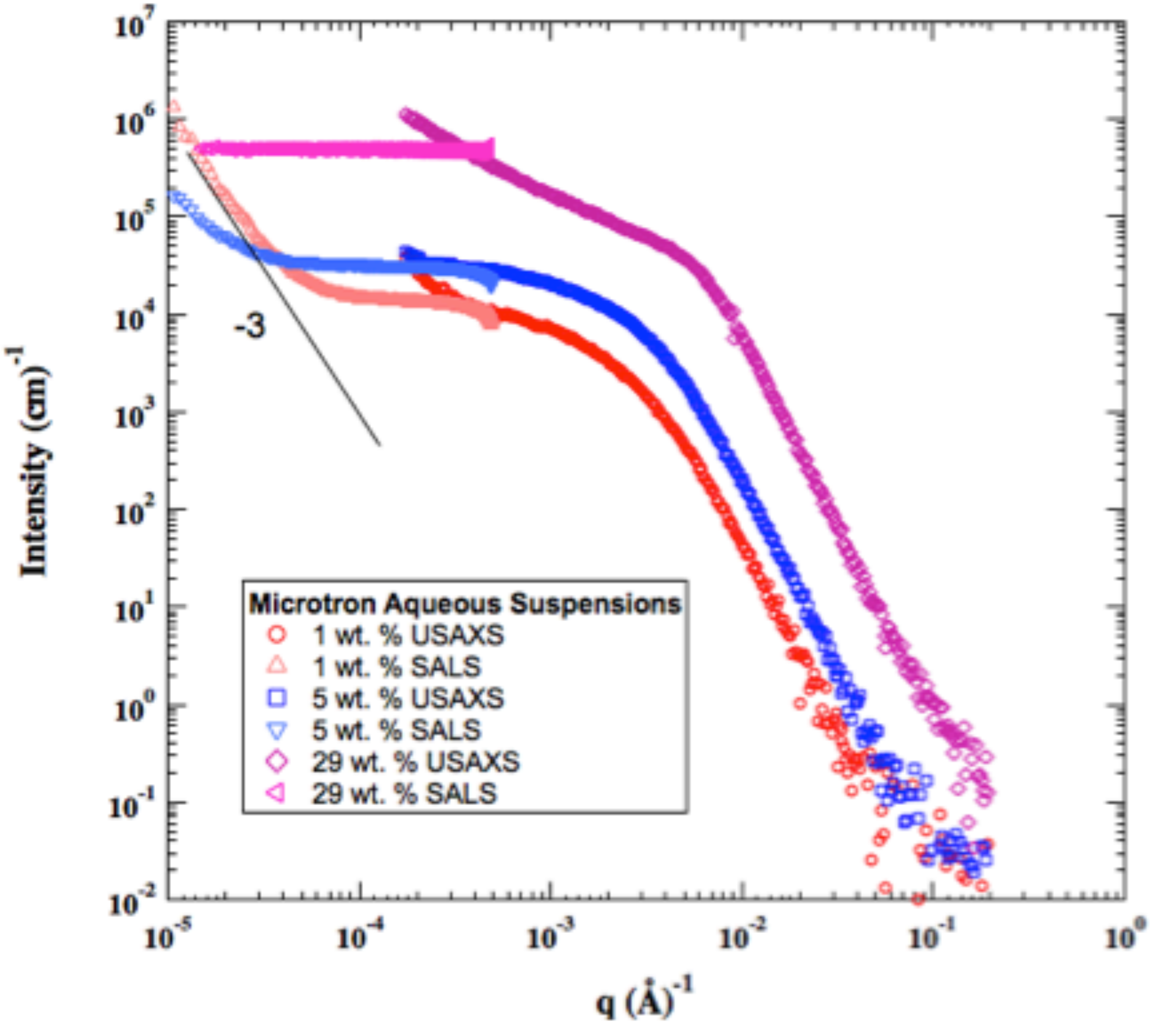

Figure 8. SALS and USAXS data from aqueous suspensions of Microtron milled pigment YFD 1123 (Yellow 14). None of the light scattering data agree with USAXS data due to contrast differences and multiple scattering for the 29 weight percent sample.

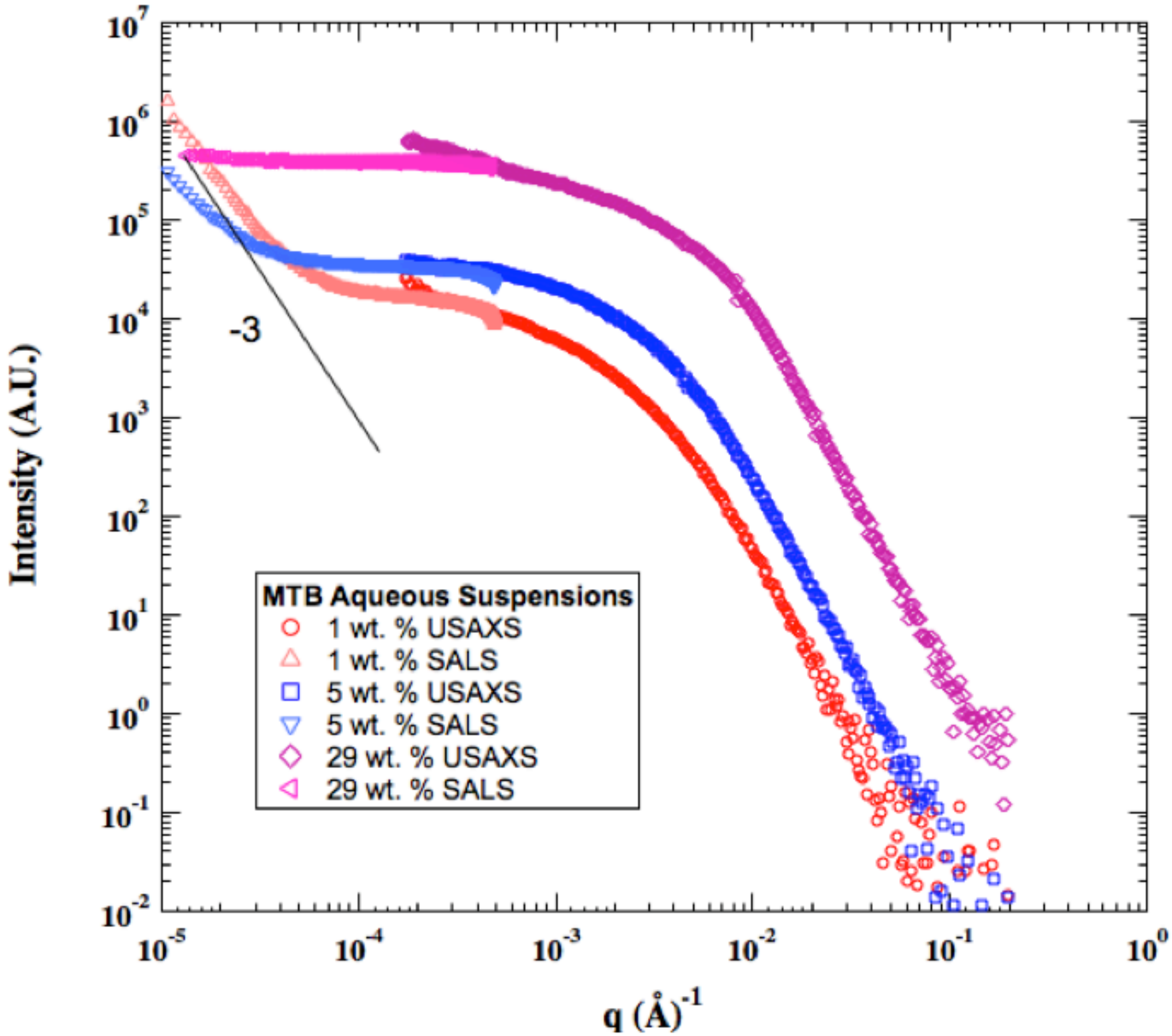

Figure 9. SALS and USAXS data from aqueous suspensions of MTB milled pigment YFD 1123 (Yellow 14). None of the light scattering data agree perfectly with the USAXS data due to contrast differences and multiple scattering for the 29 weight percent sample.

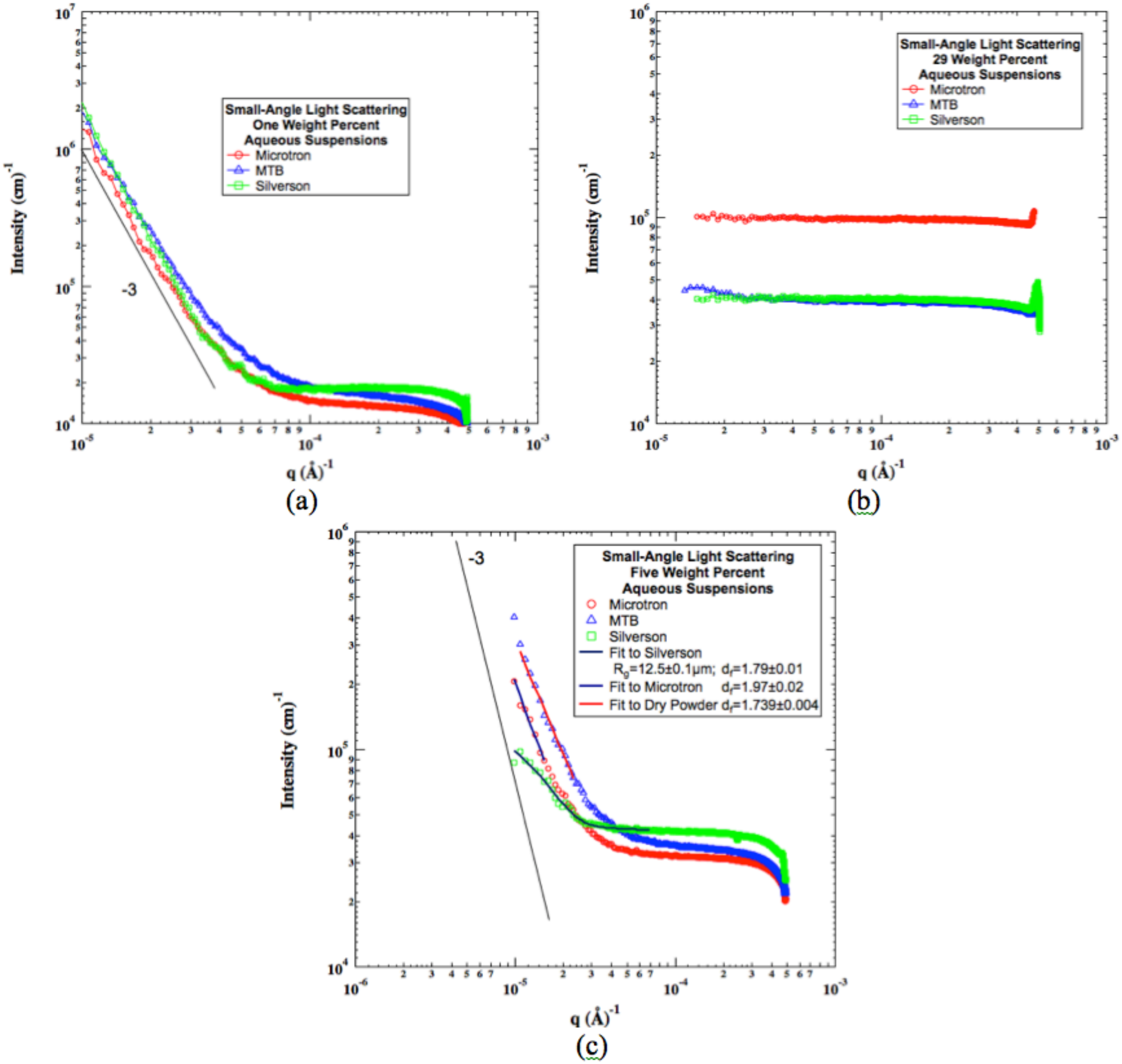

Figure 10. Comparison of SALS data from aqueous suspensions of MTB milled pigment YFD 1123 (Yellow 14). a) One weight percent samples. b) 29 weight percent samples. c) Five weight percent samples.

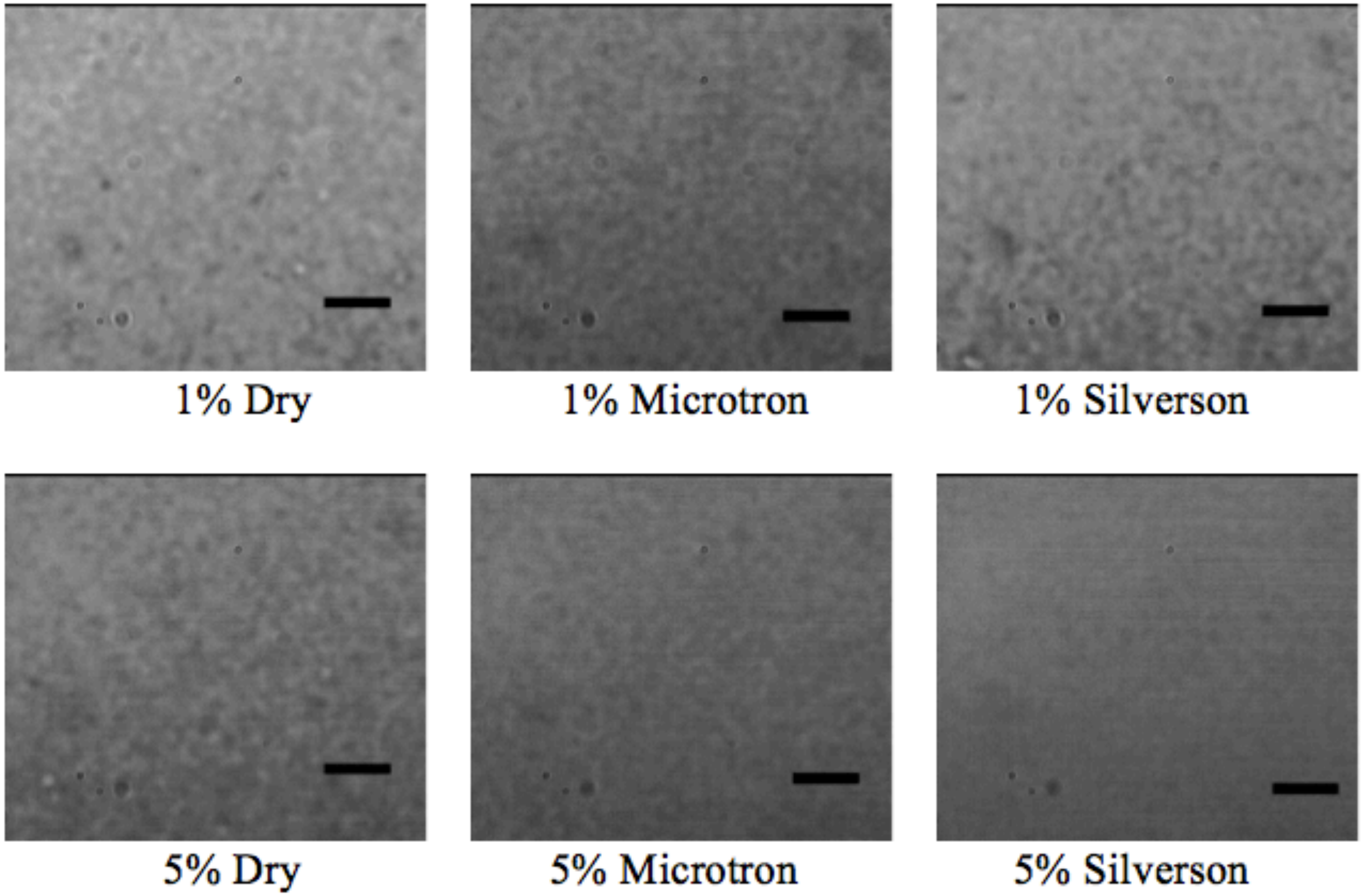

Figure 11. Optical micrographs of pigment dispersions at 500x. Bar is 10 micron. 5% Silverson sample shows a finer structure than the other 5% samples. All samples could be viewed as showing fractal-like network structures. The structure fluctuates dynamically and short videos are available for these micrographs.

http://www.eng.uc.edu/~beaucag/SunVideo/SunVideos.html

Summary:

-Yellow-14 pigment particles form aggregated structures on the nanoscale that can influence their optical performance. From past studies found large, dense aggregates (d_f ~ 2.7, and z ~ 300) are observed in polypropylene dispersions.

-In this study smaller aggregates are observed in surfactant stabilized aqueous dispersions of pigment with about 16 primary particles and a low density with a fractal dimension of 1.34 and about three branches per aggregate.

-The MTB milled sample has primary particles of 36.6 nm Sauter mean diameter. In the previous study the 5% PY14 in polypropylene sample had primary particles of about 80 nm diameter.

-The primary particle size was 60 nm for Microtron milling and 62 nm for Silverson milling. The degree of aggregation dropped to about 4 for the milled samples. The polydispersity of aggregates and primary particles was about the same for all of the aqueous dispersion samples.

-The RPA equation could describe scattering from higher concentration aqueous suspensions with some variation in the enthalpic interaction term, χ, and the volume ratio in Table 1.

Summary:

-Light scattering from the highest concentration 29% samples displayed multiple scattering and/or screening effects that were not seen for x-ray scattering. This may be related to the higher angles used in light scattering or to differences in contrast between x-rays and light. The one percent dispersions didn't match well the light scattering data in the overlapping region.

-LS for the five percent dispersions seemed to agree with USAXS data. All three of the one percent samples displayed highly polydisperse domains or clusters larger than 50 µm in light scattering. The five percent samples displayed mass fractal scattering with mass fractal dimensions of 1.7 and 2.0 for the Microtron sample. The Microtron sample also displayed 12.5 µm clusters while the other two samples displayed fractal clusters larger than 50 µm.

-Distinctions can be made between the Silverson and Microtron milled samples from the five percent light scattering data and from the one percent USAXS data. On the nanoscale, the pigment makes smaller primary particles with a lower degree of aggregation for the Microtron samples. The Silverson aggregates are probably branched to some extent though this couldn't be quantified from the USAXS data. In light scattering, the Microtron sample has much smaller clusters of fractal aggregates with a higher density and mass fractal dimension for the five percent aqueous dispersion. This is consistent with the optical micrographs shown in Figure 11.